

A new longirostrine beaked whale *Flandriacetus gijseni* gen. et sp. nov. (Ziphiidae, Cetacea, Mammalia) from the Tortonian of the North Sea Basin

Klaas Post¹, Mark Bosselaers² & Dirk Munsterman³

¹ Natural History Museum Rotterdam, Westzeedijk 345, 3015 AA Rotterdam, the Netherlands

² Institut Royal des Sciences Naturelles de Belgique, Rue Vautier 29, 1000 Brussels, Belgium

³ Netherlands Institute of Applied Geoscience TNO – Geological survey of the Netherlands, Princetonlaan 6, 3584 CB Utrecht, the Netherlands

ABSTRACT

Based on 13 more or less complete skulls and some attached postcranial elements the presence of a new longirostrine beaked whale species *Flandriacetus gijseni* gen. et sp. nov. is reported from the southern North Sea Basin. Dated by dinoflagellate cysts to 8.1–7.5 Ma (Tortonian age), the new species represents the youngest occurrence of a longirostrine stem beaked whale in the North Atlantic. The large collection allows observations on the morphological differences between some of the North European members of the Messapicetiformes clade.

Keywords Fossils, marine mammals, whale evolution, morphology, functional dentition

Cite this article Post, K., Bosselaers, M., & Munsterman, D., 2025 - A new longirostrine beaked whale *Flandriacetus gijseni* gen. et sp. nov. (Ziphiidae, Cetacea, Mammalia) from the Tortonian of the North Sea Basin - *Deinsea* 23: 1 - 31.
DOI: 10.5281/ZENODO.17880020

Submitted 16 May 2025

Revised 12 November 2025

Accepted 25 November 2025

Published 18 December 2025

Author for correspondence

klaaspost@fishcon.nl

Editors of this paper

Bram W. Langeveld

Copyright ©

2025 Post, Bosselaers & Munsterman

Distributed under Creative Commons
CC-BY 4.0

DEINSEA online

ISSN 2468-8983

INTRODUCTION

With at least 25 genera in the fossil record, the Ziphiidae represent the cetacean family with the highest past diversity (Bianucci *et al.* 2016a; Ramassamy 2016; Lambert *et al.* 2023). The extant members spend most of their lives as deep-divers in epipelagic settings. They are suction feeders (mainly targeting cephalopods), usually lack functional dentition (except *Tasmacetus shepherdi* Oliver, 1937), and possess one or two pairs of erupted or semi-erupted tusks on lower jaws that are interpreted to be tokens of sexual dimorphism, display, and intraspecific fighting (Macleod 2000; Macleod & Herman 2004; Lambert *et al.* 2010).

The present knowledge of the morphology and evolution of extinct crown ziphiids is limited and observations on tusks

and dentition are scarce. Cranial fossils of these ziphiids are excavated in Belgian, Danish, Japanese and Peruvian strata, or taken from dredging areas near Brazil, Chile, Kerguelen, Portugal, Spain, South Africa and the Netherlands (Van Bree 1997; Lambert & Louwye 2006, 2016; Bianucci *et al.* 2007, 2016a, 2023, 2024; Wijnker *et al.* 2008; Lambert *et al.* 2009; Gol'din & Vishnyakova 2013; Ichishima *et al.* 2016; Post & Bosselaers 2017; Tanaka *et al.* 2019; Ramassamy & Lauridsen 2019; Lambert *et al.* 2023). They do not show clear signs of functional dentition in maxilla and mandibula.

Stem ziphiids, however, are known in more detail. They are reported from Argentina, Belgium, Denmark, Italy, the Netherlands, Peru, Portugal, Spain and the USA (Weber 1917; Bianucci *et al.* 1992, 2010, 2013, 2016a and b, 2019; Lam-

bert 2005; Post & Bosselaers 2010; Buono & Cuzzuol 2013; Lambert *et al.* 2013, 2023; Bosselaers 2014; Ramassamy 2016; Miján *et al.* 2017; Bakker & Post 2019). Most known stem ziphiids are longirostrine and possess extensive functional dentition in upper and lower jaws, including – in the taxa where the tip of the lower jaw is preserved – one or two pairs of tusks.

The best-known stem ziphiid *Messapicetus* is currently known by two species reported from the Balearic Islands (Spain), Italy (holotype of *Messapicetus longirostris* Bianucci & Landini, 1992), Peru (holotype of *Messapicetus gregarius* Bianucci, Lambert & Post, 2010) and tentatively from the west coast of the USA (Bianucci *et al.* 1992, 1994, 2010, 2016a and b, 2019; Fuller & Godfrey 2007; Ramassamy *et al.* 2018). The fossil record of the genus confirms that at least *M. gregarius* was able to target epipelagic prey and has been recorded in large numbers at one locality, which may indicate a gregarious behaviour (Bianucci *et al.* 2010; Lambert *et al.* 2015).

All stem ziphiids with fused or joined pachyosteosclerotic premaxillae at the rostrum are grouped in a *Messapicetiformes* clade (Bianucci *et al.* 2024). The early diverging members of this clade are characterized by a longirostrine appearance (ratio of rostral length and condylobasal length between 0.6 and 0.78 – McCurry & Pyenson 2019; Lambert & Goolaerts 2022), functional dentition in upper and lower jaw, a prenarial basin, and a mandible with a long and fused symphysis with a semi-circular ventral surface ($> 1/3$ of the length of the mandible).

This article reports and describes 13 specimens of stem ziphiids from the Tortonian of the Netherlands. It presents a new genus and species *Flandriacetus gijseni* gen. et sp. nov., increases the knowledge on the morphology of the clade and highlights in detail the morphological differences with the closely related beaked whale *Ziphirostrum marginatum* du Bus, 1868. Dated to c. 8.1–7.5 Ma, it represents – together with *Dagonodum mojnium* Ramassamy, 2016 from Denmark – the most recent presence of functional dentition in stem ziphiids in the North Atlantic.

MATERIAL AND METHODS

Institutional abbreviations

IRSNB, Institut Royal des Sciences Naturelles de Belgique, Brussels, Belgium; NHG, Koninklijk Zeeuws Genootschap der Wetenschappen, Middelburg, the Netherlands; NNML (or RGM), Naturalis Biodiversity Center, Leiden, the Netherlands; NMR: Natural History Museum Rotterdam, Rotterdam, the Netherlands; MAUL, Museo dell'Ambiente, Università di Lecce, Italy; MDM, Museo Diocesà de Menorca, Menorca, Spain; MSM, Museum Sønderjylland Naturhistorie og Palæontologi, Gram Lergrav, Denmark; MUSM, Museo de Historia Natural, Universidad Nacional Mayor de San Marco, Lima, Peru; SGHN, Museo da Natureza Sociedade Galega de Historia Natural, Ferrol, Spain.

Studied specimens

The ziphiid specimens described in this article are coded with NMR numbers and were discovered in 2014, 2015, 2018,

and 2019 during fishing expeditions on the bed of the Westerschelde estuary, organised by the Natural History Museum Rotterdam (Post & Reumer 2016). They were encased in large blocks of glauconitic sandstone. Preparation of the specimens was undertaken with mechanical tools (occasionally with acid preparation of details) by one of the authors (KP) assisted by Jordi Kempers.

Specimens directly examined for comparison

Aporotus dicyrtus du Bus, 1868: IRSNB M.541 (holotype); *Aporotus recurvirostris* du Bus, 1868: IRSNB M.1887 (holotype), NMR999100159960, NMR999100159959, NMR999100159958; *Beneziphius brevirostris* Lambert, 2005: IRSNB M.1885 (holotype), IRSNB M.1886, NHG 23667; *Beneziphius cetariensis* Miján, Louwye & Lambert, 2016: SGHN MF MA0953 (holotype); *Caviziphius alti-rostris* Bianucci & Post, 2005: NNML 447230 (holotype); *Choneziphius leidy* Bianucci *et al.*, 2013: IRSNB M.188, SGHN MA0633 (holotype), SGHN MA0640, SGHN MA0641, SGHN MA0937; *Choneziphius planirostris* Duvernoy, 1851: IRSNB M.1881, IRSNB M.1882, IRSNB M.1883, IRSNB 3767–3773, IRSNB 3776, IRSNB 3779, IRSNB 3780, IRSNB 3790, NHG 22069, NHG 22773, NHG 23310, NMR999100000275, NMR999100007480, NMR999100007481, NMR999100007484, NMR999100007485, NMR999100007486, NMR999100007499, NMR999100007949, NMR999100008077, NMR999100008198, NMR999100008199, NMR999100009913, NNML ST 153415, NNML ST 153415, NNML ST 153620, NNML ST 170052, NNML ST 118478, NNML ST 20211, NNML ST 132506, NNML ST 146242, NNML ST 104557, NNML ST 12286; *Dagonodum mojnium*: MSM 1001X; *Mesoplodon europaeus* (Gervais, 1855): NMR9990001379; *Messapicetus longirostris*: MAUL no number (holotype); *Messapicetus gregarius*: MUSM 1037 (holotype), MUSM 950, MUSM 951, MUSM 1036, MUSM 1038, MUSM 1394, MUSM 1481, MUSM 1482, MUSM 1718; *Tusziphius atlanticus* Bianucci *et al.*, 2013: SGHN MA0926 (holotype), NMR999100003020 (paratype); *Ziphirostrum marginatum*: IRSNB M.1878 (holotype), IRSNB M.1874, IRSNB M.1875, IRSNB M.536, IRSNB M.537, IRSNB M.1876, IRSNB M.1877, IRSNB M.1879, NHG 22773, NHG 23310, NHG 23395, NMR999100007487, NMR999100159956; NMR999100153673, NNML ST 20121, NNML ST 20113, NNML 20779; *Ziphirostrum recurves* (du Bus, 1868): IRSNB M.544 (holotype); *Ziphirostrum turniense* du Bus, 1868: IRSNB M.539 (lectotype), IRSNB M.1880.

(*Z. marginatum* is considered the best-known member of its genus (both other species are known by rostra only), but the large number of fossils of *Z. marginatum* stored in Belgian and Dutch collections show confusing variability and characters (pers. ob. KP). For this study IRSNB 3845–M536 and NMR999100159956 are considered as the best-preserved representatives of *Z. marginatum* and used as reference.)

Anatomical terminology and measurements

Anatomical terminology follows Mead & Fordyce (2009); Lambert *et al.* (2013) and Ichishima (2016). Measurements

mainly follow Ross (1984); Lambert (2005) and Ramassamy *et al.* (2018).

Palynological analysis

Sediment samples were taken from four of the sandstone blocks with skulls. They were prepared at Palynological Laboratory Services (PLS, UK) and at the laboratory of the Geological Survey of the Netherlands (GSN-TNO, NL) using the standard sample processing procedures, which involves HCl and HF treatment, and sieving over a 15 µm mesh sieve (Janssen & Dammers 2008). The organic residue was mounted with glycerine-gelatine on microscope slides. One or two microscope slides were made of each sample: in addition to a non-oxidized kerogen slide, the organic residues were, if necessary, also oxidized with HNO₃ in order to concentrate the palynomorphs and reduce the abundant “Structureless Organic Matter” (SOM). The palynological analysis was carried out at the GSN-TNO according to standard procedures. The microscope slide was counted as the TNO standard until an initial minimum of 200 palynomorphs (spores, pollen and dinoflagellate cysts) had been identified (when present). The remainder of the slides were successively scanned (at least a minimum of 200 specimens) for rarer taxa. Miscellaneous fossils (e.g. freshwater *Pediastrum*, and fresh to brackish water *Botryococcus*) were also quantitatively and relatively (to the palynomorph sum) counted, but kept outside the total sum of 200 specimens of dinocysts, spores and pollen. Together a total average number of approximately 200–250 microfossils is reached, statistically sufficient for indicating the dominant dinocyst species fluctuation (Brinkhuis *et al.* 2003). Diagnostic species are discussed in the next section, and a complete distribution chart including all species found is given as an appendix. The age interpretation is based on the Last Occurrence Datum (LOD) and First Occurrence Datum (FOD) of dinoflagellate cysts. For the dinoflagellate cyst taxonomy the so-called “Lentin and Williams index” is followed (Fensome *et al.* 2019). Palynological interpretation is based on key references concerning the palynostratigraphy of the Neogene from the North Sea region such as: Powell (1992); Louwye *et al.* (2004); Munsterman & Brinkhuis (2004); Kuhlmann *et al.* (2006); Dybkjaer & Piasecki (2010); Louwye & De Schepper (2010); Köthe (2012) and Munsterman *et al.* (2019). The Geological Time Scale 2016 is used (Ogg *et al.* 2016). Dinoflagellate cyst zones are referred to Munsterman & Brinkhuis (2004) recalibrated to Ogg *et al.* (2016) in Munsterman *et al.* (2019) (Appendix 1).

Nomenclatural Act

The electronic version of this article in Portable Document Format (PDF) will represent a published work according to the International Commission on Zoological Nomenclature (ICZN), and hence the new names contained in the electronic version are effectively published under that Code from the electronic edition alone. This published work and the nomenclatural acts it contains have been registered in ZooBank, the online registration system for the ICZN. The ZooBank LSIDs (Life Science Identifiers) can be resolved and the associated information viewed through any standard web browser by

appending the LSID to the prefix <https://zoobank.org/>. The LSID for this publication is: 73EDD1DB-4521-4090-87B2-F22033B62F11. The online version of this work is archived and available from the following digital repository <https://zenodo.org/>.

Cladistic analysis

A cladistic analysis was performed in PAUP 4.0a - 169 (Swoford 2002) based on the list of characters and the matrix for the cladistic analysis of Ziphiidae of Bianucci *et al.* (2024) (Appendix 2). We included in our analysis the 15 species of the Messapicetiformes-clade of Bianucci *et al.* (2024) – being all the ziphiid species most closely related to *Flandriacetus* gen. nov., the basal stem ziphiids *Notoziphius bruneti* Buono & Cuzzuol, 2013 and *Ninoziphius platyrostris* de Muizon, 1983, and two basal odontocete species (*Squalodon bellunensis* Dal Piaz, 1901 and *Squaloziphius emlongi* de Muizon, 1991). Including *Flandriacetus gijseni* gen. et sp. nov. (with 47 of the 59 characters scored), the matrix contains 20 species (Appendix 3). The character scores of *Dagonodum mojunum* (direct observation of the type specimen during a visit to Denmark (pers. ob. KP); Char 1: 0=1) and *Tusciziphius atlanticus* (based on the type specimen and the paratype; Char 13: 2=1; 14: 1=0; 47: ?=1, 48: 0=1) were slightly adjusted from Bianucci *et al.* (2024) (Appendix 3). We performed an heuristic search of 25,000 replicates. All characters are treated as unordered, have equal weight, with no topological constraints in effect.

GEOLOGICAL CONTEXT AND PALYNOLOGICAL INTERPRETATION

The evolution and origin of the North Sea Basin is based on ongoing post-rift thermal subsidence since mid-Cretaceous times and the progressive opening of the northern Atlantic Ocean and African-Eurasian collision. These factors resulted in regional uplift of the British Isles, Fennoscandian Shield, Ardennes, Rhenish and Bohemian massifs during the Paleogene-Neogene. The present-day country of the Netherlands is located on the southern margin of the North Sea Basin. Uplift along the Weald-Artois Axis has led to interim closure of the Channel Seaway (Knox *et al.* 2010), linking the North Sea Basin to the eastern Atlantic, furthermore isolating the basin during the late Miocene. Lithospheric folding is associated with increased subsidence of the Roer Valley Graben already in the late Miocene (Deckers & Louwye 2020). Regional uplift in the Tortonian instigated the development of the proto-Rhine fluvial-deltaic depositional system of the Inden Formation in Germany and the south-eastern part of the Netherlands (Schäfer *et al.* 2005). The Inden Formation is followed by the Kiezeloollite Formation in the latest Tortonian and younger (Munsterman *et al.* 2019). These fluvial systems caused increased the nutrient concentration of the water. The Inden and Kiezeloollite Formations are westward transitional to the marine Diessen Formation. A gradual cooling trend between 9.5 and 7.4 Ma was recorded in the southern North Sea Basin (Donders *et al.* 2009).

All our material of *Flandriacetus gijseni* gen. et sp. nov. orig-



Figure 1 Location of site 6D, Westerschelde river, Zeeland province, the Netherlands (A + C present, B during the Late Miocene).

inates from a very limited site in the Westerschelde river (Fig. 1) and is embedded in a dense sandy glauconitic matrix from the Diessen Formation, a lithostratigraphic unit which includes Tortonian to Messinian strata (Munsterman *et al.* 2019). The Diessen Formation was deposited in a predominantly shallow to open marine environment. The sediments were deposited as prodeltaic. Along the edges of the distribution area, nearshore settings occur (Munsterman *et al.* 2019).

The age dating is not based on the cetacean fossils, but on microfossils from the (partly cemented) sands attached to the fossils. The cementation of the otherwise unconsolidated sands is considered to have occurred during fossilization. The preservation and yielding of the palynomorph assemblages (dinoflagellate cysts, spores and pollen) is moderate (NMR999100012016) to good (NMR999100012017, NMR999100014034) to very good (NMR999100016765). Bisaccate pollen dominate the sporomorphs. Bisaccate pollen are formed by conifers, gymnosperms (Gymnospermae). Bisaccates have a relatively higher aerial and aquatic buoyancy than other sporomorphs, and may indicate a relatively distal position from the coast and/or increased fluvial influence in a marine basin (Abbink 1998). The marine dinoflagellate cyst assemblage is variegated, showing neritic conditions. The most common species are: *Achomosphaera andalousiense*, *Amiculosphaera umbracula*, *Barssidinium graminosum*, *Habibacysta tectata*, *Labyrinthodinium truncatum*, *Lejeunecysta* sp., *Lingulodinium machaerophorum*, *Melitisphaeridium choanophorum*, *Operculodinium centricarpum*, *Operculodinium* spp., *Reticulosphaera actinocoronata*, *Selenopemphix brevispinosa*, *Selenopemphix dionaeacysta*, *Spiniferites* spp. and

Trinovantedinium spp. The chronostratigraphic diagnostic taxa are: *Gramocysta verricula*, *Hystrichosphaeropsis obscura*, *Impagidinium 'densiverrucosum'*, *Labyrinthodinium truncatum*, and *Selenopemphix armageddonensis*. The former four taxa together have a minimum age in the Late Miocene, Tortonian. Taxa present with a maximum age range in the Tortonian are: *Impagidinium 'densiverrucosum'* and *Selenopemphix armageddonensis*. In addition, *Achomosphaera andalousiense* has a slightly extended first occurrence in the late(st) Serravallian (Munsterman & Brinkhuis 2004). The current assemblages fit into the Late Miocene, late Tortonian SNSM 14 Zone, dated to 8.1-7.5 Ma (Munsterman & Brinkhuis (2004), recalibrated to the geological time scale of Ogg *et al.* (2016) in Munsterman *et al.* (2019). This zone is correlated to the *Hystrichosphaeropsis obscura* Biozone of Denmark (Dybækjær & Piasecki 2010), and the DN9 Zone of the eastern USA and Germany (De Verteuil & Norris 1996; Köthe 2012). Zone SNSM 14 is defined by the LOD of *Labyrinthodinium truncatum* and the LOD of *Systematophora (Cleistosphaeridium) placacantha*. The latter taxon is not recorded. Diagnostic marker species for the Middle Miocene (SNSM zones 5-11) and early to mid-Late Miocene (SNSM zones 12-13) are missing in the palynomorph spectra.

Dinoflagellate cysts analysis provided the relative age of the matrix of four of the described beaked whale crania to be late Tortonian, Zone SNSM 14; which yields an age of 8.1-7.5 Ma (Appendix 4).

SYSTEMATIC PALEONTOLOGY

CETACEA Brisson, 1762

ODONTOCETI Flower, 1867

ZIPHIIDAE Gray, 1850

FLANDRIACETUS gen. nov.

Type species (by original designation): *Flandriacetus gijseni* gen. et sp. nov. (monotypic) from the Netherlands

FLANDRIACETUS GIJSENI gen. et sp. nov.

Holotype – NMR999100012016: well-preserved almost complete skull, rostrum, partial mandibles and six vertebrae (cervical vertebra 1-5, one anterior thoracic vertebra); missing the apex of rostrum, apex of the mandibles, ear bones and teeth (Fig. 2). To be mentioned hereafter as NMR12016.

Referred specimens – NMR999100012017: partial cranium and rostrum, the vertex is somewhat distorted and separating parts of the frontals, left premaxillary crest and supraoccipital. NMR999100014034: partial cranium, rostrum and (possibly) a fragment of a hyoid (thyrohyal), missing the anterior part of the rostrum, ear bones, teeth and the upper part of the braincase (exposing the brain cavity). NMR999100016769: partial cranium, rostrum and a single detached tooth, missing the apex of the rostrum and ear bones. NMR999100159955: partial skull, rostrum and a fragment of the symphysis of the mandible, missing the anterior part of the rostrum, ear bones and teeth. NMR999100198032: well-preserved almost complete skull, rostrum and mandibles, missing the pterygoid, apex of ro-

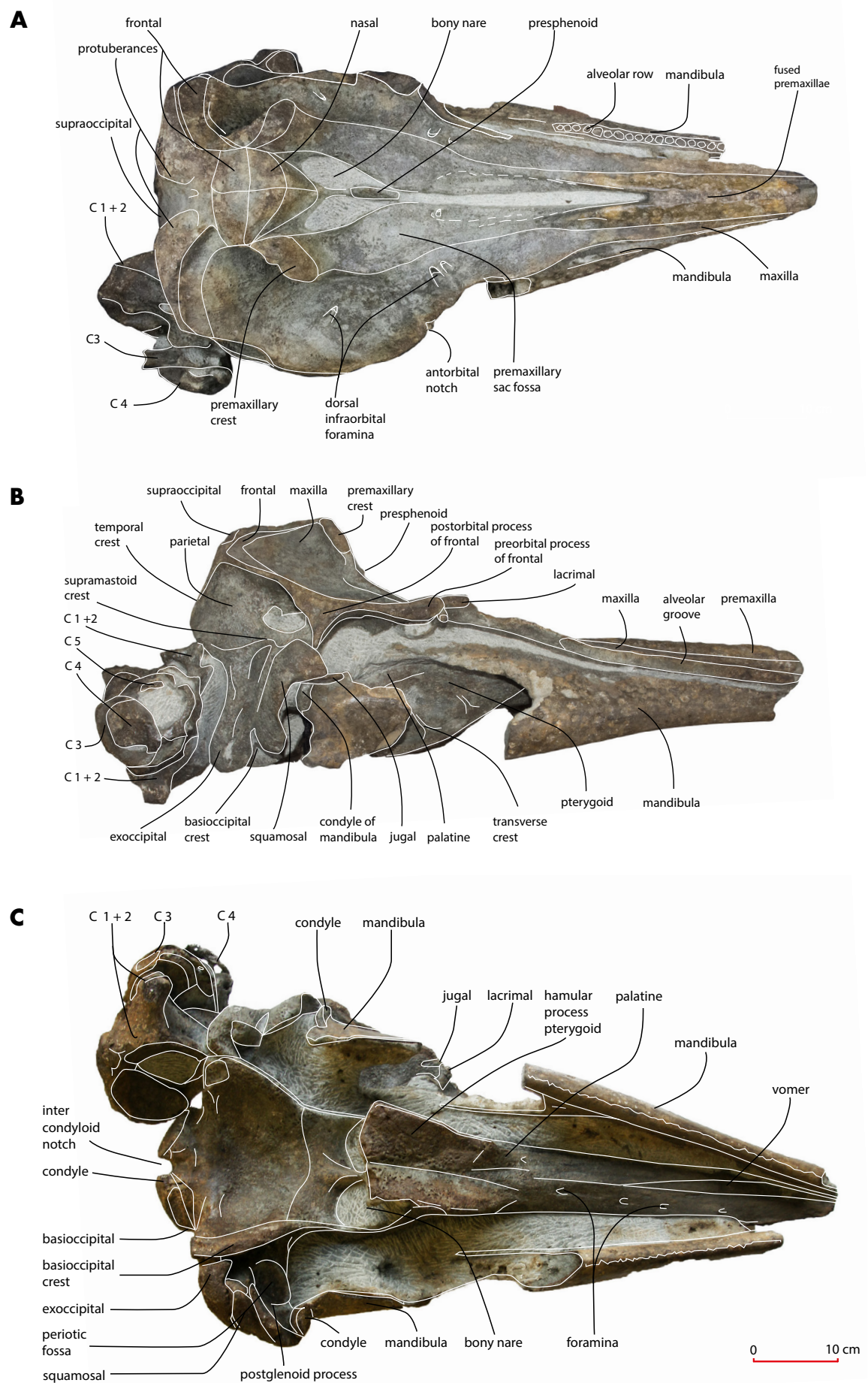


Figure 2 NMR999100012016, holotype cranium of *Flandriacetus gijseni* gen. et sp. nov., dorsal (A), lateral (B), ventral view (C).

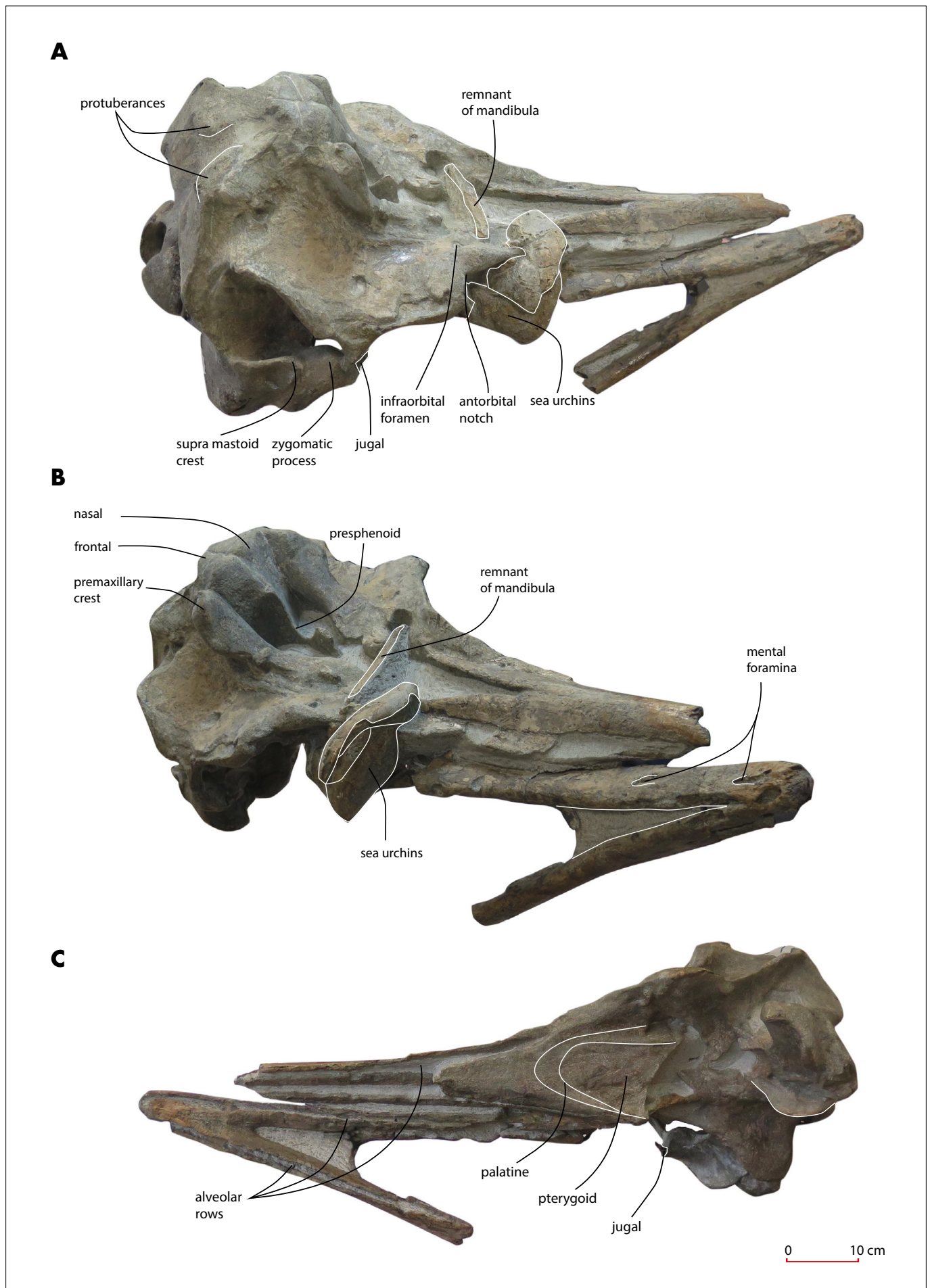


Figure 3 NMR999100198032, cranium of *Flandriacetus gijseni* gen. et sp. nov., dorsolateral (A), anterolateral (B), lateroventral view (C).

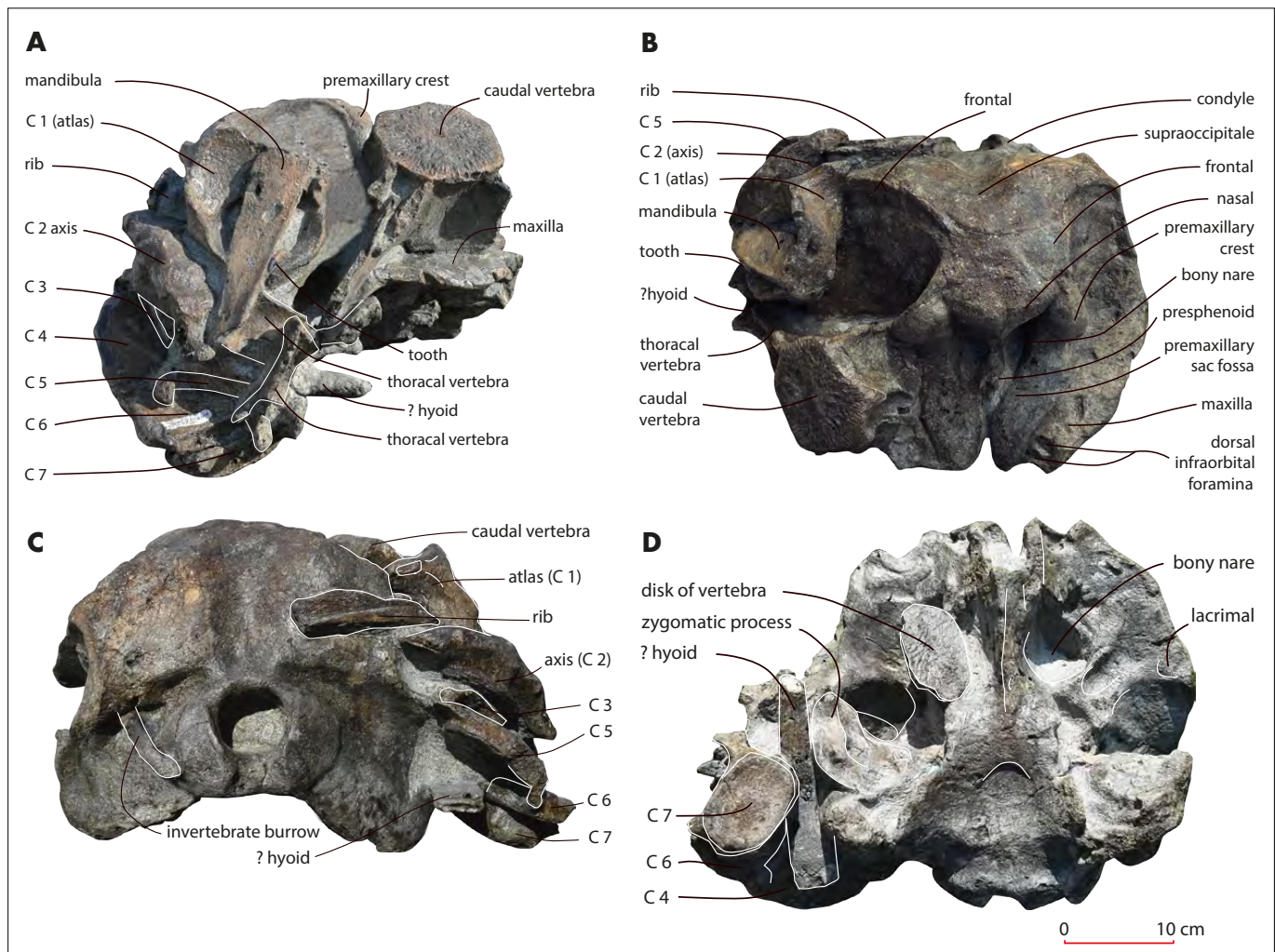


Figure 4 NMR999100016765, *Flandriacetus* gen. nov. sp. nov., lateral (A), dorsal (B), caudal (C), ventral view (D).

trum, apex of the mandibles, ear bones and teeth. Some large sea-urchins and bivalves are attached to the skull (Fig. 3). NMR999100205260: partial skull (with jugal) and rostrum, missing the apex of the rostrum, ear bones and teeth. The supraoccipital is somewhat distorted causing the squamosa to reach over and above the maxillae. NMR999100205266: partial skull and base of the rostrum; missing the left squamosal, ear bones and teeth. NMR999100212995: partial skull, rostrum and fragment of a left mandible, missing supraoccipital, squamosa and apex of the rostrum. To be mentioned hereafter as NMR12017, NMR14034, NMR159955, NMR16769, NMR198032, NMR205260, NMR205266 and NMR212995.

Referred specimens named as *Flandriacetus* gen. nov. sp. - Specimens from the same site, of the same age and with preserved elements which are morphologically identical to *F. gijseni* gen. et sp. nov., but either not complete enough, or showing some elements which prevent (as yet) a 100% secure assignment to *F. gijseni* gen. et sp. nov. NMR999100016464: vertex with fragments of premaxillary crests; NMR999100016765: skull with fragments of a mandible, four detached teeth, eleven vertebrae (cervical vertebra 1-7, three anterior thoracic vertebrae and one caudal verte-

bra), two fragments of ribs, missing the rostrum and ear bones (Fig. 4); NMR999100212990: vertex with left premaxillary crest; NMR999100212991: vertex with attached fragments of maxillae. To be mentioned hereafter as NMR16464, NMR16765, NMR212990, NMR212991.

Etymology – *Flandria* from the Latin name of the Belgian region of Vlaanderen and the Dutch province Zeeuws-Vlaanderen, which border the estuary of the Westerschelde river; *cetus* is Latin for whale. *Gijseni* in honor of Bert Gijsen, for decades of carefully collecting, documenting and preserving cetacean fossils from Vlaanderen – saving them for scientific research.

Locality – All specimens were taken by Natural History Museum Rotterdam expeditions from the bed of the Westerschelde estuary (Zeeland province, the Netherlands), at a depth of c. 28 metres, around position 51°21'569"N-03°54'251"E (Westerschelde locality 6D; Post & Reumer (2016)) (Fig. 1).

Horizon and age – All specimens are embedded in a dense sandy glauconitic matrix originating from the Diessen Formation – widespread at the site which includes Tortonian to Messinian strata (Munsterman *et al.* 2019). Dinoflagellate cysts determined the matrix to be of Tortonian age 8.1-7.5 Ma (Munsterman 2017a and b; Appendix 4). The sediment

of NMR12016 contained some molluscs and brachiopods that corroborate this dating (Appendix 5). From the same site and the same lithological unit – besides numerous articulated postcrania – fossils were recovered of at least 18 (partial) crania of balaenopterids and cetotheres, a single cranium of a pontoporiid, associated vertebrae of a basking shark, a single vertebra of a large pinniped, and a large shield of a leather-back turtle. Mostly dated to the same geological interval as the beaked whales (Zone SNSM 14), but some slightly older (SNSM 13 – 8.8-8.1 Ma) (Post & Reumer 2016; Post *et al.* 2017; Munsterman 2017a, 2017b; Bisconti *et al.* 2019; Marx *et al.* 2019; Peters *et al.* 2019).

Diagnosis – *F. gijseni* gen. et sp. nov. is a large longirostrine, beaked whale bearing functional teeth, typified by the unique combination of the following measurements and characters: bizygomatic width of the cranium (BZW) 331-370 mm; premaxillae dorsally fused until separating at least 200 mm anterior to the base of the rostrum – showing a significant posterior portion of the mesorostral groove; maxilla separated from the nuchal crest by a wide strip of frontal; rostrum base dominated by a long and wide prenarial basin; top of the presphenoid above the surface of the premaxillae; one large dorsal antorbital foramen usually combined with a second significantly smaller foramen; a moderately elevated, slightly asymmetric, leftwards oriented vertex not overhanging the external bony nares; anterior-most tip of the nasal located c. 50 mm below the surface of the vertex.

Differential diagnosis – Cranial synapomorphies (elevated vertex with transverse premaxillary crests, wide hamular fossa of the pterygoid sinus extending anteriorly beyond the level of the antorbital notch and ventrally beyond the ventral level of the basicranium, and transverse crests on the inner surface of the hamular process (only known in some ziphiid species (Lambert 2013)), confirm *F. gijseni* gen. et sp. nov. as a member of the Ziphiidae (Bianucci *et al.* 2016a). The anteroposterior shortening of the zygomatic process of the squamosal; the ventral margin of the postglenoid process of the squamosal located clearly more dorsally than the ventral margin of the paraoccipital process of the exoccipital; and the presence of a precoronoid crest on the dorsal margin of the mandible, corroborate this assignment.

Within the Ziphiidae, the Messapicetiformes are stem ziphiids diagnosed by two synapomorphies: 1) mesorostral groove roofed by the dorsomedial contact or fusion of the premaxillae (character 3 – Appendix 2), and 2) pachyosteo-sclerotic development of the premaxillae along the rostrum (character 30 – Appendix 2) (Bianucci *et al.* 2024). Both synapomorphies are noted in *F. gijseni* gen. et sp. nov.

Within the Messapicetiformes, *F. gijseni* gen. et sp. nov. differs from *Notoziphius bruneti* Buono & Cozzuol, 2013 by: nasals on the vertex more wide than long, longer and more massive frontals on the vertex, large prenarial basin, longer dorsal exposure of the mesorostral groove on the rostrum; from *Chimuziphius coloradensis* Bianucci *et al.*, 2016 by: large dorsal exposure of the frontals on the vertex, absence of a large maxillary crest, large prenarial basin, and extended dorsal exposure of the mesorostral groove on the rostrum; from *Aporotus recurvirostris* and *A. dicyrtus* by: fused pre-

maxillae (rather than tightly joined premaxillae) which are not medially inflated, more extended dorsal exposure of the posterior portion of the mesorostral groove, and functional maxillary dentition; from *Beneziphius brevirostris*, *B. cetariensis*, *Choneziphius planirostris* and *C. leidy* by: much longer rostrum, more extended dorsal exposure of the posterior portion of the mesorostral groove, lack of maxillary excrescences, and functional maxillary dentition; from *Caviziphius altirostris*, *Globicetus hiberus* Bianucci *et al.*, 2013, *Imocetus piscatus* Bianucci *et al.*, 2013, *Tusciziphius crispus* Bianucci, 1997 and *T. atlanticus* by: lacking maxillary domes or rostral surface structures, elongated rostrum, more extended dorsal exposure of the posterior portion of the mesorostral groove, and functional maxillary dentition; from *Dagonodum mojnun* by: nasals on vertex not medially and posteriorly inserted into frontals, large and wide prenarial basin, and fused atlas and axis; from *Ziphirostrum marginatum* by: moderately elevated vertex, anteroposteriorly shorter nasals and longer frontals on vertex, anterior point of nasals located significantly below vertex level, apex of vertex not overhanging bony nares, large and wide prenarial basin, lack of coronoid crest, one large and one smaller dorsal infraorbital foramen at base of the rostrum, functional dentition in maxilla, more extended dorsal exposure of posterior portion of mesorostral groove, and elongated rostrum; from *Messapicetus gregarius* by: overall larger and more robust cranium (BZW 331-370 mm); lack of coronoid crest; one large and one smaller dorsal infraorbital foramen at base of rostrum; longer dorsally open posterior portion over mesorostral groove (231 mm-254 mm); slightly square or round roots of teeth; and fused atlas and axis; from *Messapicetus longirostris* by: overall larger and more robust skull - not longer than wide, distinct supramastoid crest of squamosal, longer dorsally open posterior portion over mesorostral groove (231 mm-254 mm), and alveolar row of mandible with oval or round alveoli.

COMPARATIVE DESCRIPTION

This description is based on NMR12016 (Fig. 2), NMR198032 (Fig. 3), NMR16765 (Fig. 4), and – where and if necessary – on additional information from referred specimens (Figs. 5, 6). Measurements are noted in Table 1.

Premaxilla – The anterior-most portion of the premaxilla at the rostrum is not preserved in any of the specimens. On the preserved anterior segments of the rostrum, the premaxillae are dorsomedially elevated and fused, covering a deep mesorostral groove. The fused premaxillae cover the mesorostral groove, but split anterior to the base of the rostrum, creating a dorsally open posterior portion of the groove. In NMR198032 and NMR212995 the fused premaxillae show a slightly convex surface, while in NMR12016 the surface is semi-triangular. The dorsally open portion is preserved for 231-254 mm in NMR12016, NMR212995, NMR159955, NMR198032 and NMR205266. The rostrum of the other skulls is too damaged to measure the length of this feature. The separated right and left premaxilla develop after c. 100 mm, and still anterior to the premaxillary sac fossae, into ventromedially directed parts of a wide prenarial basin (Fig. 2A). This basin is present in *Messapicetus* and *Ziphirostrum* but

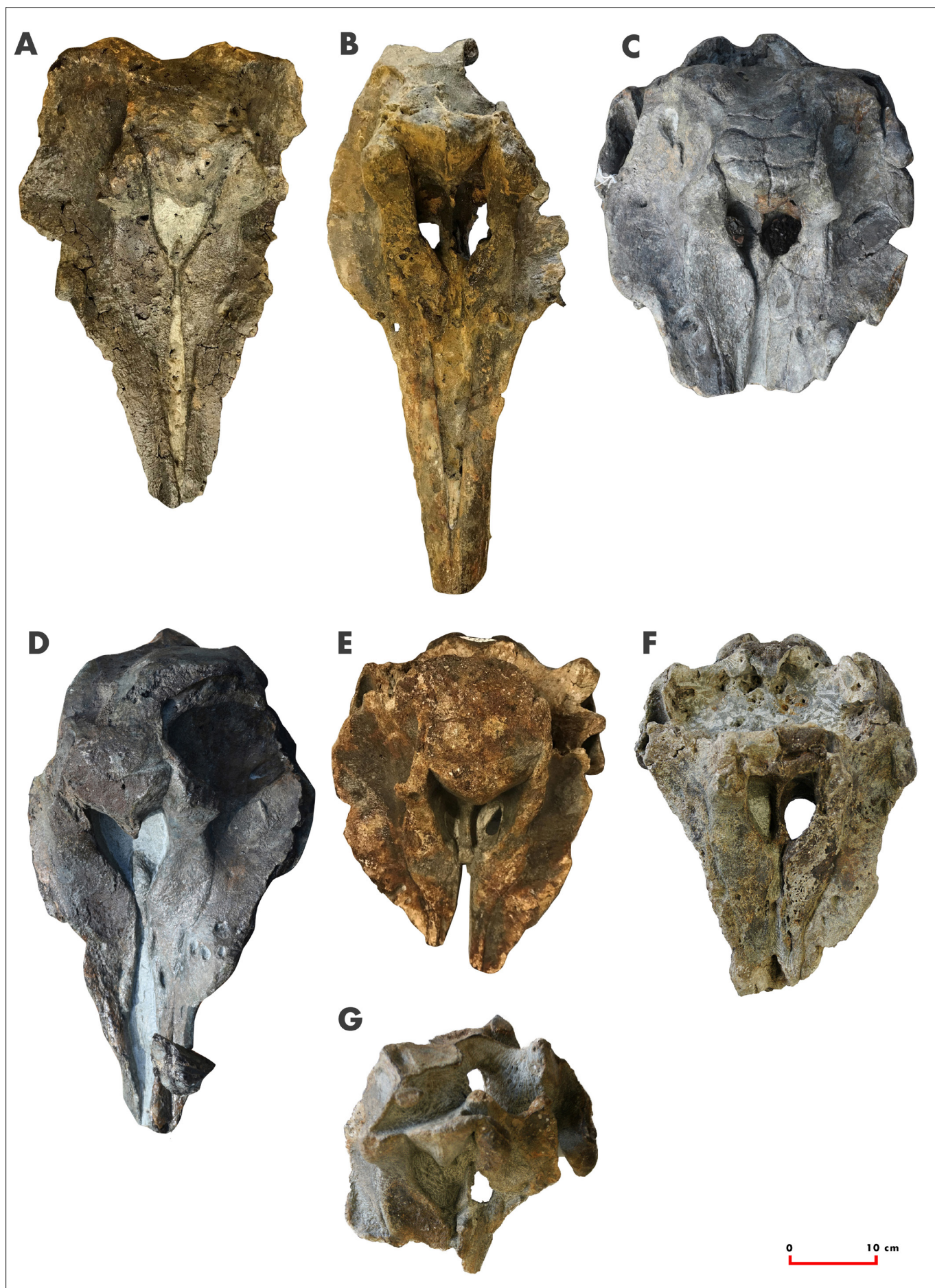


Figure 5 NMR999100205266 (A), NMR999100212995 (B), NMR999100205260 (C), NMR999100155995 (D), NMR999100016769 (E), NMR999100014034 (F) and NMR999100012017 (G), *Flandriacetus gijseni* gen. et sp. nov., dorsal views.

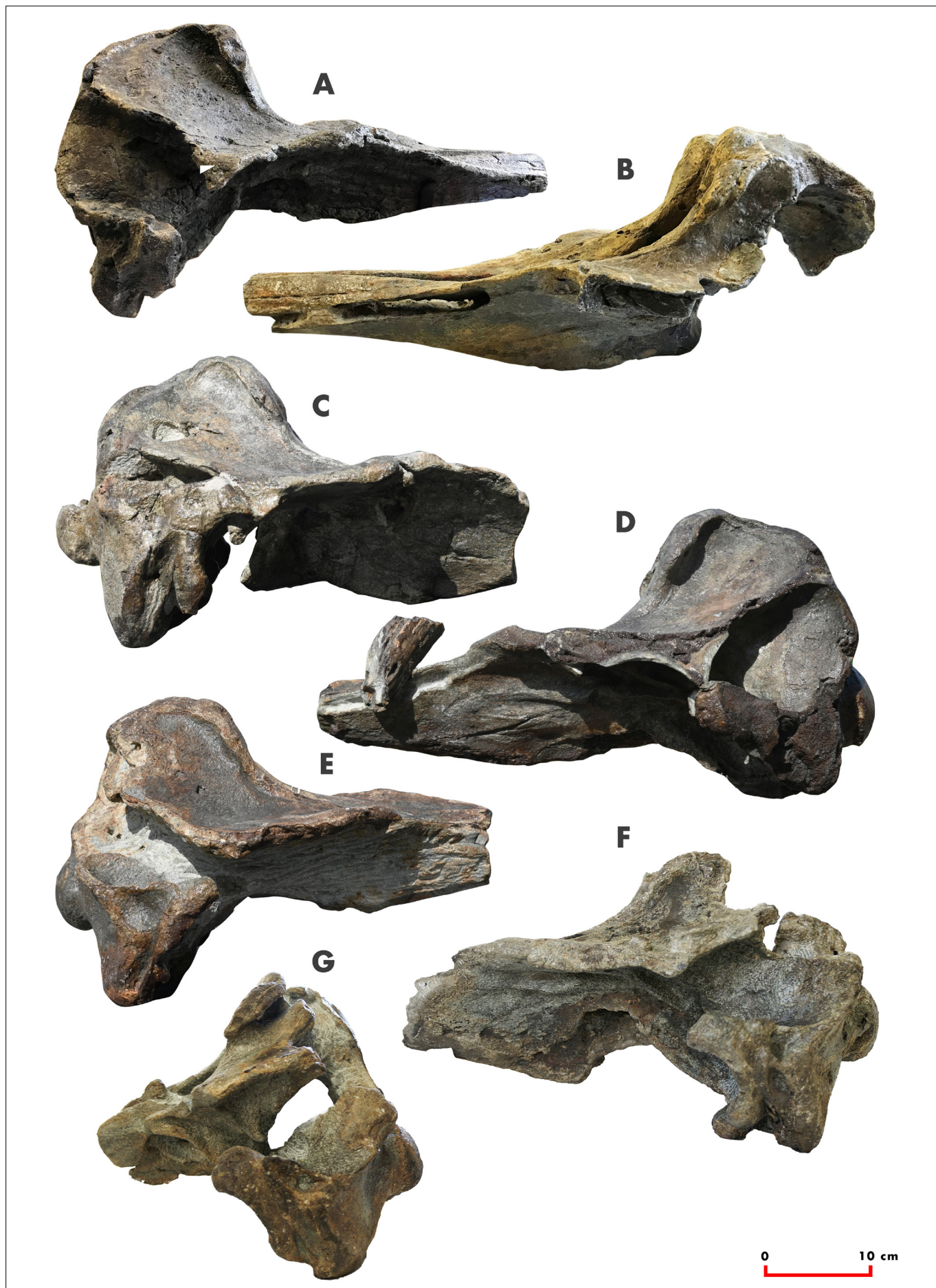


Figure 6 NMR999100205266 (A), NMR999100212995 (B), NMR999100205260 (C), NMR999100155995 (D), NMR999100016769 (E), NMR999100014034 (F) and NMR999100012017 (G), *Flandriacetus gijseni* gen. et sp. nov., lateral views.

NMR	12016	12017	14034	16765	16769	159955	198032	205260	205266	212995
Condylbasal length	>733	>326	>419	>355	>408	>519	>768	>396	>526	>602
Width rostrum at fusion of premaxillae	-	-	-	-	-	-	112	-	e84	76
Depth rostrum at fusion of premaxillae	-	-	-	-	-	-	-	-	51	62
Minimum distance between maxillae at rostrum base	135	-	e119	96	131	e126	130	137	124	133
Width rostrum base at antorbital notch	e247	-	e222	e208	e230	e240	248	236	e232	222
Depth rostrum at rostrum base	-	-	112	-	104	98	85/130	103	>91	e82
Dorsal infraorbital foramina at left rostrum base	2	-	2	2	2	4	1	1	1	2
Dorsal infraorbital foramina at right rostrum base	2	-	1	1	2	-	e1	4	2	2
Length ms-rostral groove from rostral base/antorbital notch till fusion	238	-	-	-	-	-	251	-	231	254
Bizygomatic width	364	e370	348	e338	331	333	354	338	e344	-
Maximum width over premaxillary sac fossae	151	-	138	153	e141	153	143	151	134	154
Maximum width right premaxillary sac fossa	78	79	65	73	>57	72	60	73	63	67
Maximum width left premaxillary sac fossa	57	-	59	61	57	69	e53	64	55	61
Maximum width bony nares	71	e74	70	74	79	72	78	76	57	75
Maximum elevation presphenoid over premaxilla	16	18	-	22	-	-	29	11	-	-
Minimum width ascending process right premaxilla	40	43	40	e38	26	e41	e28	38	40	40
Minimum width ascending process left premaxilla	34	-	e31	33	e21	34	31	24	30	33
Transverse width over premaxillary crests	168	176	-	176	-	164	179	164	e168	177
Width right premaxillary crest	51	60	-	56	-	-	53	51	e56	49
Width left premaxillary crest	47	e43	-	46	-	47	47	43	44	50
Maximum width nasals	85	90	e84	101	92	-	101	87	83	98
Minimum posterior distance of maxillae on vertex	100	e110	-	89	92	76	e92	94	103	e97
Length of medial suture of frontals on vertex	33	-	>37	-	38	-	31	19	34	29
Height of supraoccipital between vertex and foramen magnum	161	e172	-	159	129	154	181	-	158	-
Maximum width between protuberances on supraoccipital	48	-	-	e88	-	e72	e98	62	42	e98
Minimum distance between temporal fossae in posterior view	211	-	e210	e228	-	212	182	-	216	-
Transverse width of occipital condyles	127	-	129	132	126	e118	132	-	112	-
Height left condyle	81	e70	72	79	77	81	77	-	68	-
Width left condyle	48	e42	47	53	43	49	50	-	40	-
Width foramen magnum	48	-	59	57	55	-	51	-	52	-
Distance between jugular notches	188	-	184	168	172	e170	182	184	-	-
Length of pterygoid hamulus	183	-	-	-	-	-	-	-	-	-
Maximum width of pterygoid hamulus	>94	-	-	-	92	-	e85	-	-	-
Length of pterygoid	-	-	-	-	>138	166	e178	-	126	e195
Extension of pterygoid on rostrum (from base rostrum)	-	-	-	-	>118	>95	e143	-	69	e149
Height zygomatic of squamosal	119	121	95	-	103	e129	96	103	-	-
Length of mandible	>565	-	-	>214	-	>108	>623	-	-	>109
Maximum height of mandible	e134	-	-	-	-	-	>94	-	-	>106
Distance between mandibular condyle and alveolar row	386	-	-	-	-	-	-	-	-	-
Height of mandibular condyle	52	-	-	-	-	-	-	-	-	50
Width of mandible at fusion of symphysis	-	-	-	-	-	-	68	-	-	-
Height of mandible at fusion of symphysis	-	-	-	-	-	-	47	-	-	-

Table 1 Measurements of *Flandriacetus gijnseni* gen. et sp. nov.: NMR999100012016 (holotype), NMR999100012017, NMR999100014034, NMR999100016765, NMR999100016769, NMR999100159955, NMR999100198032, NMR999100205260, NMR999100205266 and NMR999100212995 in mm; - = no data, > = larger than, e = close to.

absent in *D. mojunum*. The premaxillary sac fossae are slightly concave to flat and asymmetric (left distinctly narrower than right and occasionally a bit more elevated). Premaxillary foramina cannot easily be detected, NMR12016 shows a small foramen on the right side and NMR159955 shows a transversely narrow foramen on both sides (16 mm anterior to the rostrum base). The posterior part of the lateral border of the premaxillary sac fossa is elevated from the maxilla. The ascending process is medially constricted. At its smallest point the constriction of the left process is c. 25% narrower than the right one. It rises gradually towards a moderately thickened, anterolaterally directed, slightly convex, premaxillary crest whose posterior edge reaches the nasal on the vertex.

Maxilla – The anterior-most portion of the maxilla is not preserved in any of the specimens. On the rostrum the preserved dorsal part of the maxilla is present as a wide laterally oriented and convex massive bone. At the rostrum base the maxilla reaches a maximum width of 101 mm (NMR14034). A clear prominent notch is lacking (unlike *M. gregarius* and *Z. marginatum*). The lateral border develops, just before the antorbital notch, into a slightly pointed but not prominent ridge (NMR12018, NMR205260, NMR205266) or weakly convex bulge (NMR14034, NMR159955, NMR198032). The overall architecture of this area resembles, albeit less prominently, the structure noted in *Chavinziphius* (Bianucci *et al.* 2016a). Usually two dorsal infraorbital foramina (one large and one small) are located on each side medially from the antorbital notch and along and just in front of the maxillary ridge or bulge. However, in some specimens 1-2 additional much smaller foramina are noted (NMR159955, NMR205260). At c. 100-110 mm posterior to the antorbital notch another small dorsal infraorbital foramen is located. After this foramen the maxilla rises posteromedially gradually and gently to the vertex and nuchal crest, a significant difference with *Z.*

marginatum where the maxilla abruptly and almost vertically rises to the nuchal crest. In all specimens the maxilla remains separated from the nuchal crest by a broad strip of exposed frontal (Fig. 2A, 4B).

The preserved anterior-most ventral parts of the maxilla of NMR12016 show a 241 mm marked but eroded alveolar row with remains of the base of circular 7 x 7 mm alveoli.

Presphenoid and cribriform plate – At the location where the dorsally open but narrow mesorostral groove distinctively widens into the bony nares, an abruptly dorsally elevated, massive and pointed presphenoid separates the bony nares (Fig. 2A, 3B, 4B). The pointed dorsal edge of a bulb - up to 52 mm long and 16 mm wide - towers up to 21 mm over and above the surface of the premaxillary sac fossae. This elevated structure is in lateral view visible as a sharply pointed triangle in line with, or just before the anterior surface of the ascending process of the premaxillae. In the large sample of *M. gregarius* this feature is only noted – albeit in a very limited way - in MUSM 1036. The presphenoid proceeds then as a narrow ridge between the nares and evolves into a wide cribriform plate.

Nasal – The dorsal surface of the triangularly shaped nasals is flat. They are wider than long. At 83-101 mm wide, they are wider than observed in *M. longirostris* (c. 66-70 mm), but equal to *M. gregarius* (c. 86-102 mm, Bianucci *et al.* 2010). The nasals are not medially posteriorly wedged into the frontals, as in *D. mojunum*. The anterior border has a weakly convex surface and which is pointed at the midline. However, the anterior-most point of the nasals is located more ventrally at c. 50 mm below the dorsal surface and on top of the suture with the cribriform plate. In lateral view this point of the nasals is more or less reaching the front of the ascending process of the premaxilla. In both *Messapicetus* species the anterior-most tip of the nasal is also located at a significant distance below

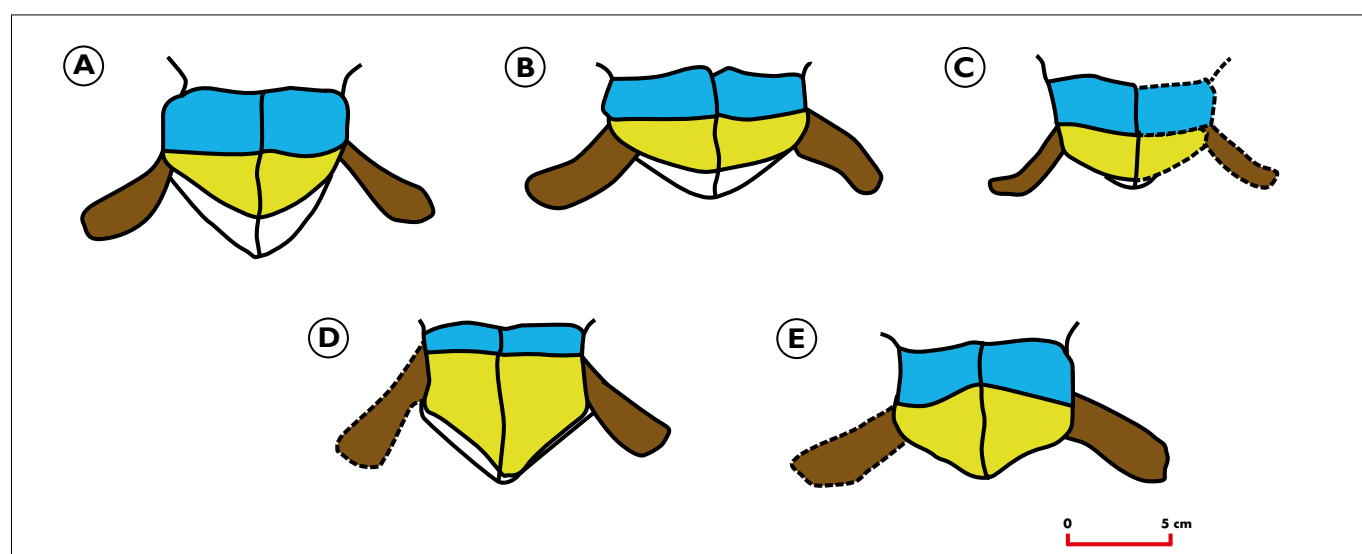


Figure 7 Schematic drawing of vertex of *Flandriacetus gijseni* gen. et sp. nov. – NMR999100012016 (A), *Messapicetus gregarius* – adjusted from Bianucci *et al.* (2010) (B), *Messapicetus longirostris* - adjusted from Bianucci *et al.* (2016) (C), *Ziphirostrum marginatum* - NMR999100159956 (D), *Dagonodum mojunum* - adjusted from Ramassamy (2016) (E). (Blue – frontals, yellow & white – nasals, brown – premaxillary crests)

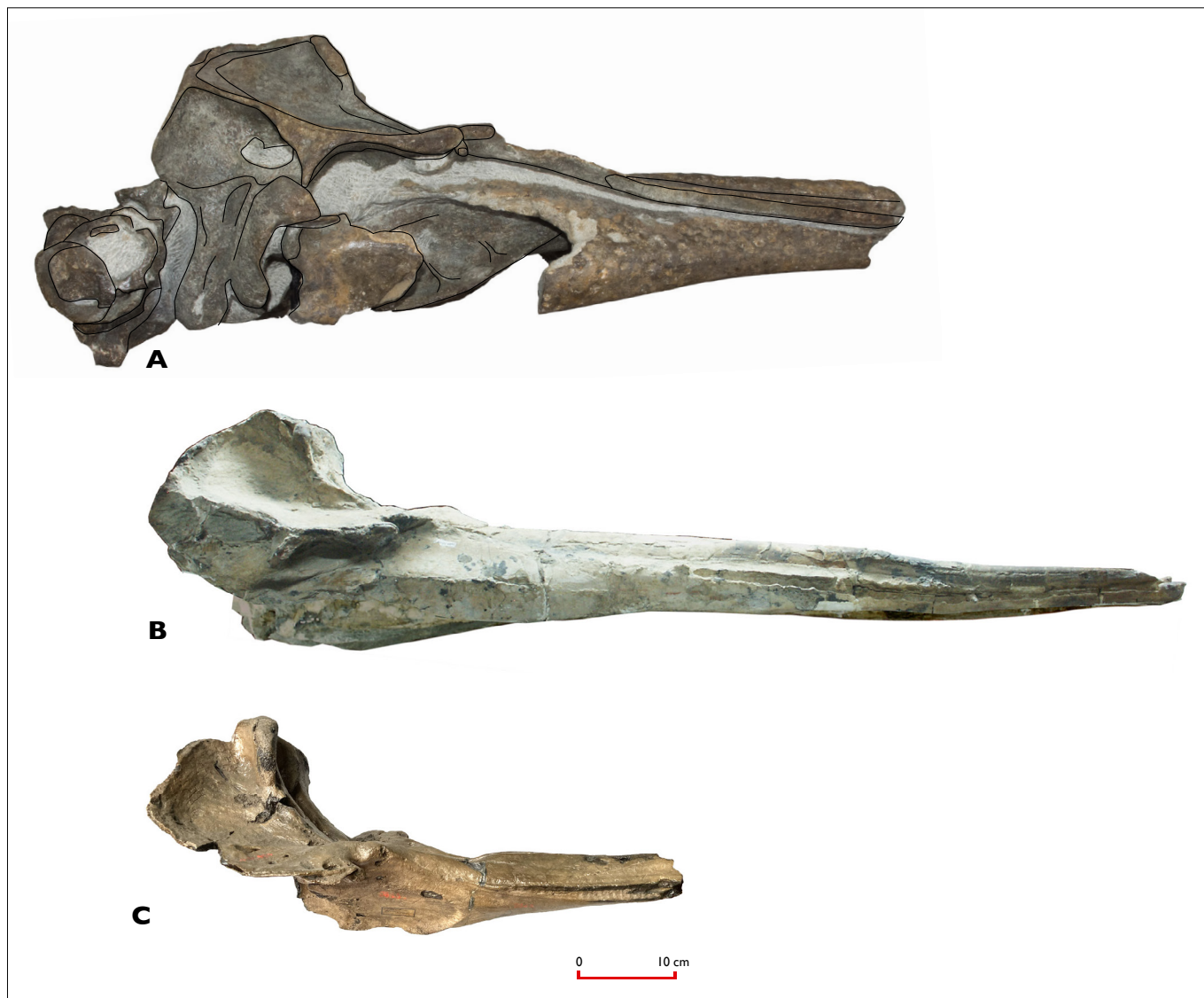


Figure 8 Lateral view of holotype cranium of *Flandriacetus gijseni* gen. et sp. nov. NMR999100012016 (A), *Messapicetus gregarius* MUSM 1037 (B), *Ziphirostrum marginatum* - IRSBN 3845 M536 (C). (G. Bianucci (B)/O. Lambert (C))

the vertex surface, but in *Z. marginatum* it is located closer to the dorsal surface of the nasals (11 mm in NMR159956).

Frontal – On the vertex, the frontals are feebly trapezoid-shaped and wider than long. The suture with the nasals is straight and in most of the specimens wider than the suture with the supraoccipital posteriorly. The latter seems to vary with the degree of narrowing between the maxillae at the nuchal crest. This variation causes the shape of frontals on the vertex to vary from semi square (NMR16769) to feebly trapezoid (NMR12016). From the vertex to the postorbital process the frontal is exposed between the nuchal crest and the posterior-most border of the maxilla as a 22-35 mm wide strip of bone (Fig. 2A, 4B). In NMR12017 (the largest specimen) this is slightly less prominent than in the other specimens. This exposed strip of frontal is present in all Westerschelde specimens and only occasionally noted (albeit feebly) in *Messapicetus*. The postorbital process is slender, directed vertically, and contacts the zygomatic process of the squamosal. In lateral view this contact point is located

posterior to the premaxillary crests. The preorbital process is not markedly thickened and is anteriorly oriented.

Vertex – The vertex of *F. gijseni* gen. et sp. nov. differs in size and some aspects of the architecture from the vertex of *M. gregarius*, *Dagonodum mojunum* and – especially – from *Z. marginatum* (Fig. 7). On the vertex, the frontals of *F. gijseni* gen. et sp. nov. (29-38 mm), *M. gregarius* (c. 29 mm) and *M. longirostris* (c. 30 mm) are significantly longer than in *Z. marginatum* (18-22 mm). Moreover, the distance from the top of the vertex to the base of the rostrum in *F. gijseni* gen. et sp. nov. (average 101 mm) is less than in *Z. marginatum* (147-155mm) (Fig. 8).

Lacrimojugal – In NMR12016 the left lacrimal is located slightly in front of the preorbital process of the frontal. The jugal is fused with the lacrimal and posteroventrally preserved as a 26 mm long, 7 mm wide, thin bone. A posterior segment of 32 mm of the right jugal is oriented towards the dorsal area of the squamosal and connects as a 30 mm wide flat shield with the anterior-most point of the zygomatic process (NMR12016 – Fig. 2B).

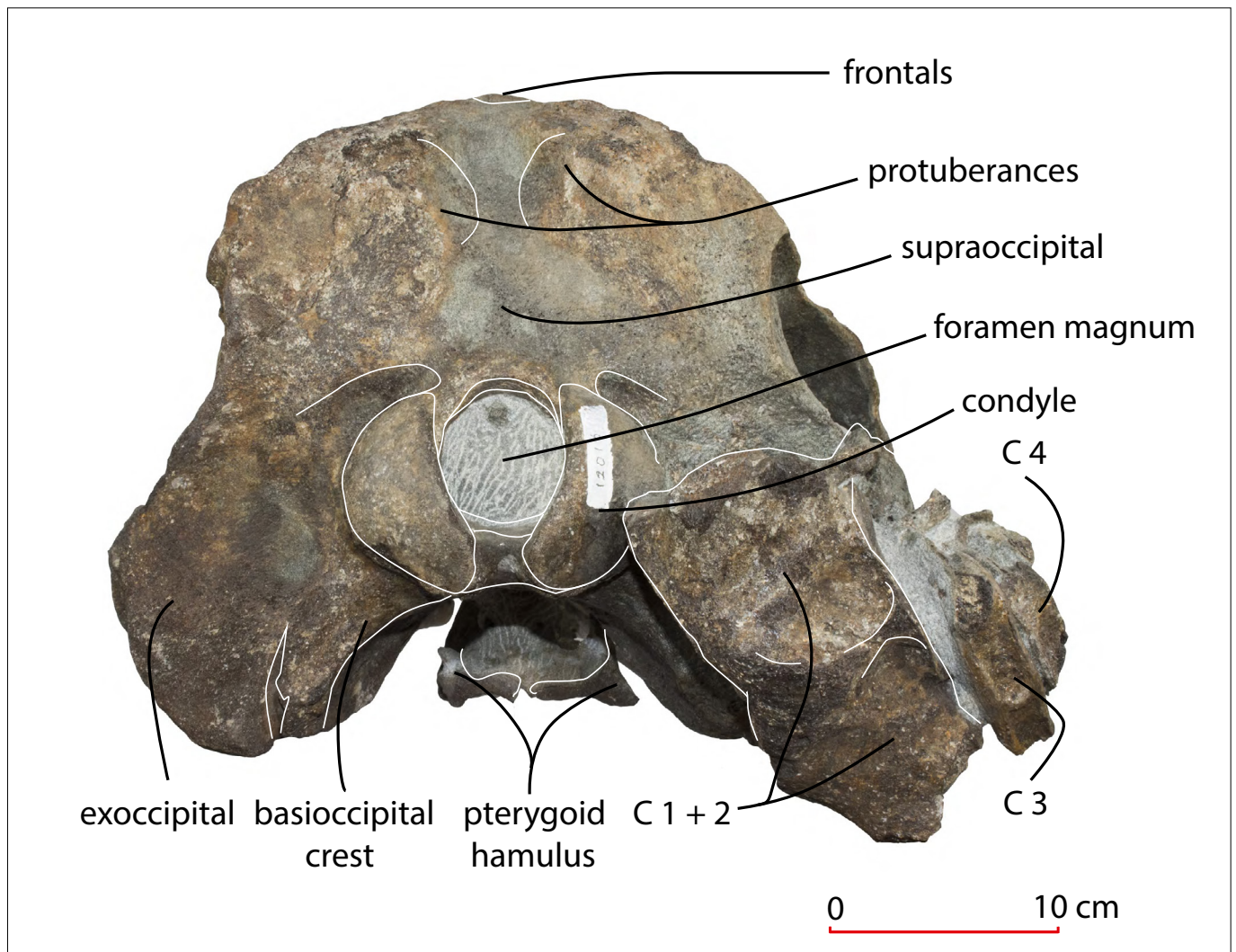


Figure 9 Holotype cranium NMR999100012016, *Flandriacetus gijnseni* gen. et sp. nov., caudal view.

Supraoccipital – In posterior view, the elevated posterior border of the vertex and the solid and massive nuchal crest marks the somewhat trapezoid-like shape of the supraoccipital (Fig. 9). The top of the supraoccipital is often located slightly lower, and is somewhat more constricted, than the frontals on the vertex. In posterior view in all specimens the dorso-medial area of the supraoccipital is strongly concave and flanked on each side by large semi-circular protuberances. Similar structures (but positioned more ventrally and much less pronounced) are noted in some individuals of *M. gregarius* and have been interpreted as a base for the attachment of the semispinalis capitus (Bianucci *et al.* 2010).

Exoccipital – The massive occipital condyles are rounded, pronouncedly convex in lateral view, and enclose a wide and circular foramen magnum. The condyles are dorsolaterally margined by a deep dorsal condyloid fossa. The paraoccipital process is massive and rounded. The ventral-most part of the exoccipital is positioned markedly more ventrally than the condyles and reaches a significantly lower ventral position than the exoccipitals in *M. gregarius*.

Basioccipital – The basioccipital crests are large and pronounced, but not thick. In ventral view both crests incline

towards each other at an angle of c. 47°, differing from *M. gregarius* (c. 40°) and closer to the angle in all extant ziphiids and of other fossil ziphiids in which this feature is preserved and described (Bianucci *et al.* 2010).

Vomer – The vomer is separated from the basioccipital/basisphenoid by a slightly upheaved choana and is visible up to the ventral part of the internal bony nares. At about mid-length of the preserved ventral part of the rostrum a small palatal part of the vomer separates the maxillae.

Parietal – All the studied specimens in which the parietal or a large part of the parietal is preserved, show an oval area of missing bone (see Fig. 2B, Fig. 6). The possible cause of this lack of bone or damage is not clear.

Squamosal – The zygomatic process of the squamosal is anterodorsally oriented, higher than long (as in all ziphiids), and positioned dorsally to the postglenoid process and the posttympanic process (however not as elevated as in extant *Mesoplodon* species). In lateral view, in the specimens where the zygomatic process is preserved, the squamosal shows a marked and rounded supramastoid crest or flange which reaches as high as, or above the top of the zygomatic process. The supramastoid crest marks the dorsal margin of

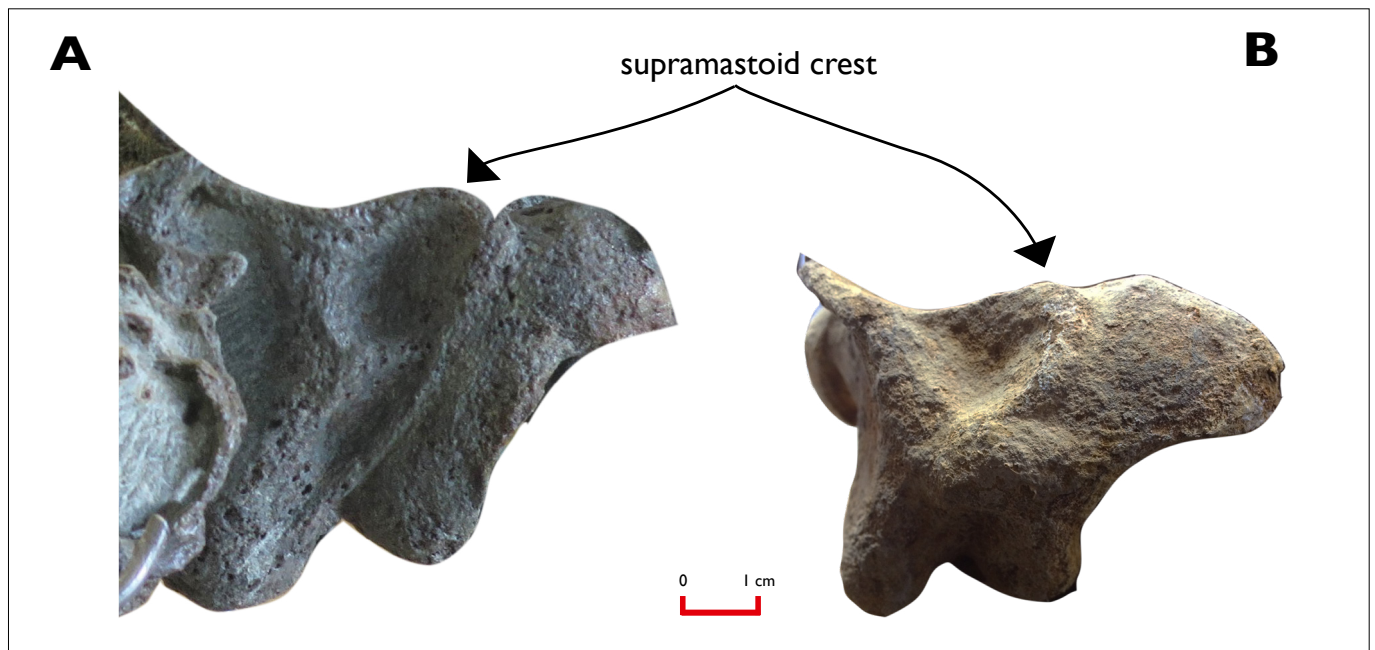


Figure 10 Lateral view of right squamosals of holotype cranium of *Flandriacetus gijnseni* gen. et sp. nov. - NMR999100012016 (A) and *Messapicetus gregarius* MUSM 1481 (B).

a large sternomastoid fossa. A similar crest is noted in one of the specimens of *M. gregarius* (MUSM 1481) (Fig. 10). Squamosa are not preserved in the holotype of *M. longirostris* and in the studied specimens of *Z. marginatum* (Bianucci *et al.* 1992; Lambert 2005); a distinct supramastoid crest seems to be lacking in all other known ziphiid taxa. The dorsal margin of the zygomatic process is profoundly rounded and swollen. In ventral view there is a large tympanosquamosal recess. In lateral view, the zygomatic process of the squamosal does not extend beyond the nasal, unlike *M. gregarius*. The height of the zygomatic process varies from 121 mm (NMR12017, with BZW of 370 mm) to 94 mm (NMR14034, with BZW of 348 mm).

Pterygoid – The hamular process of the pterygoid covers parts of the choanes and has a vast hamular fossa which excavates basically the entire process. The hamular process extends ventrally as in all extant ziphiids. The palatal surface of the pterygoid hamulus is medially inclined and V-shaped (Fig. 9). In lateral view the pterygoid shows two marked dorsoventrally oriented transverse crests (Fig. 2B). The anterior tip of the pterygoid extends on the rostrum beyond the antorbital notch.

Palatine – The palatine is exposed for some part on top of the pterygoid hamulus and on the ventral base of the rostrum. Ventrally on the rostrum it extends anterior to the antorbital notch, in NMR14034 surpassing the antorbital notch for at least 100 mm.

Mandible – The preserved posterior part of the ramus of NMR12016 measures 554 mm and is 37 mm high and 26 mm wide at the anterior break. The anterior part of the ramus and the symphysis are not preserved. The cross section of the ramus shows a rounded ventral outline. The dorsal surface shows a c. 160 mm long, broad, deep, alveolar row with faint traces

of oval alveoli of c. 8 mm long and c. 7 mm wide. The alveoli seem to differ from the anteroposteriorly enlarged mandibular alveoli of *M. longirostris* (Bianucci *et al.* 2016b). The precoronoid crest starts immediately after the alveolar row. The mandible reaches a height of c. 134 mm at the level of the antorbital notch. The crest evolves into a 11 mm wide, fairly massive, coronoid process. The massive mandibular condyle is located 52 mm below the posterior margin of the mandible and has a height of 48 mm. The process, and condyle are also present in NMR212995. The condyle is located at c. mid height of the ramus of the mandible and much more pronounced and solid than in the observed extant species of the genus *Mesoplodon*. A marked constriction links the condyle with the angular process. This constriction is shared with *Ninoziphius* and some specimens of *Tasmacetus* (Lambert *et al.* 2013), but is not present in *Chavinziphius* (Bianucci *et al.* 2016a).

Although in NMR198032 the posterior and anterior parts of the mandibles are not preserved, 586 mm of the right ramus and 424 mm of the left ramus are present. They have a fused symphysis, at least 132 mm long, which originally must have been much longer. On the right ramus two mental foramina are located 67 mm behind, and 38 mm anterior to the posterior border of the symphysis. On the left ramus they are located 18 mm behind, and 16 mm anterior to the posterior border. A mental foramen is also present in NMR159955, but the preserved fragment of the symphysis is too fragmented to ascertain its exact position.

Teeth – The preserved teeth are small and slender with an oval to round single root and an enamel crown (Fig. 11). One of the teeth of NMR16765 is 23.2 mm high (including the pointed enamel cusp of 10.4 mm), anteroposterior 10.1 mm long (at the root), and has a lingual-buccal width of 7.9 mm. One of the teeth of NMR16765 shows an occlusal wear facet

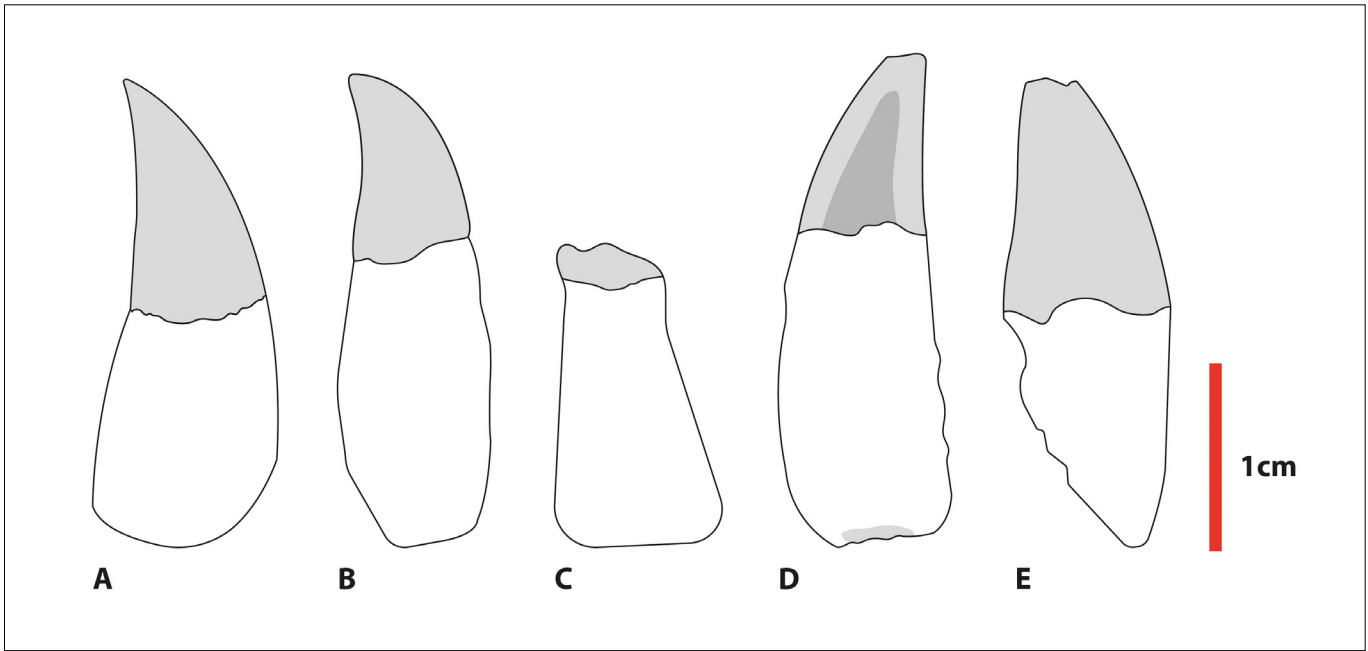


Figure 11 Teeth of NMR999100016765 - *Flandriacetus* gen. nov. sp. (A, B, C, D) and NMR999100016769 - *Flandriacetus gijseni* gen. et sp. nov. (E).

	NMR 12016	NMR 16765	MUSM 2548	MSM 1001x
Atlas		56 x 202 x -		e38 x 158 x -
Atlas/axis complex	87x 198 x 138			
Axis		48 x 178 x -	12 x 186 x -	
C3	23 x >88 x 106	21 x 148 x -		28 x - x e54
C4	25 x >79 x -	22 x - x -		
C5		22 x - x 58	21 x - x -	22 x - x e71
C6		26 x 121 x 60		28 x - x >66
C7		20 x 150 x 66	28 x - x -	
e T1	38 x 102 x >125		37 x 162 x 54	29 x - x 63
e T4		61 x 108 x 49		
e Ca 6		96 x >126 x e105		

Table 2 Measurements of vertebrae of NMR NMR999100012016 (holotype), NMR NMR999100016765 (*Flandriacetus gijseni* gen. et sp. nov.), MUSM 2548 (*Messapicetus gregarius*) and MSM 1001 (*Dagonodum mojunum*); Length centrum x width at level transverse processes x posterior height of centrum. In mm, - = no data, > = larger than, e = close to.

and abraded tip (Fig. 11D). Similar facets are noted in teeth of *Dagonodum* in which they are supposed to have an attrition origin (Ramassamy 2016). Although the limited sample of teeth does not allow clear conclusions, the teeth differ from *M. gregarius* where all teeth show anteroposteriorly enlarged, transversely flattened roots (Bianucci *et al.* 2010) and *D. mojunum*, in which the teeth are more or less similar in size but have broad solid square roots fitting into square alveoli (Ramassamy 2016).

Vertebrae – In NMR12016 five cervical vertebrae and an anterior thoracic vertebra are preserved posterior and lateral

to the foramen magnum (Fig. 12). The atlas and axis vertebrae are completely fused as in *Ninoziphius* (Lambert *et al.* 2013; Ramassamy *et al.* 2018). The transverse process is massive and semi-circular. The neural spine is posteriorly elongated. The posterior surface presents two postzygapophyses. C3 is positioned directly behind the atlas/axis complex, and fits perfectly to the posterior vertebral body of the complex. C4 is behind and close to C3, severely damaged, but still complete enough to be measured. Only a fragment of C5 has been preserved, which prevents any observation. The ventral surfaces of C1-C3 show prominent excavations and a ventral

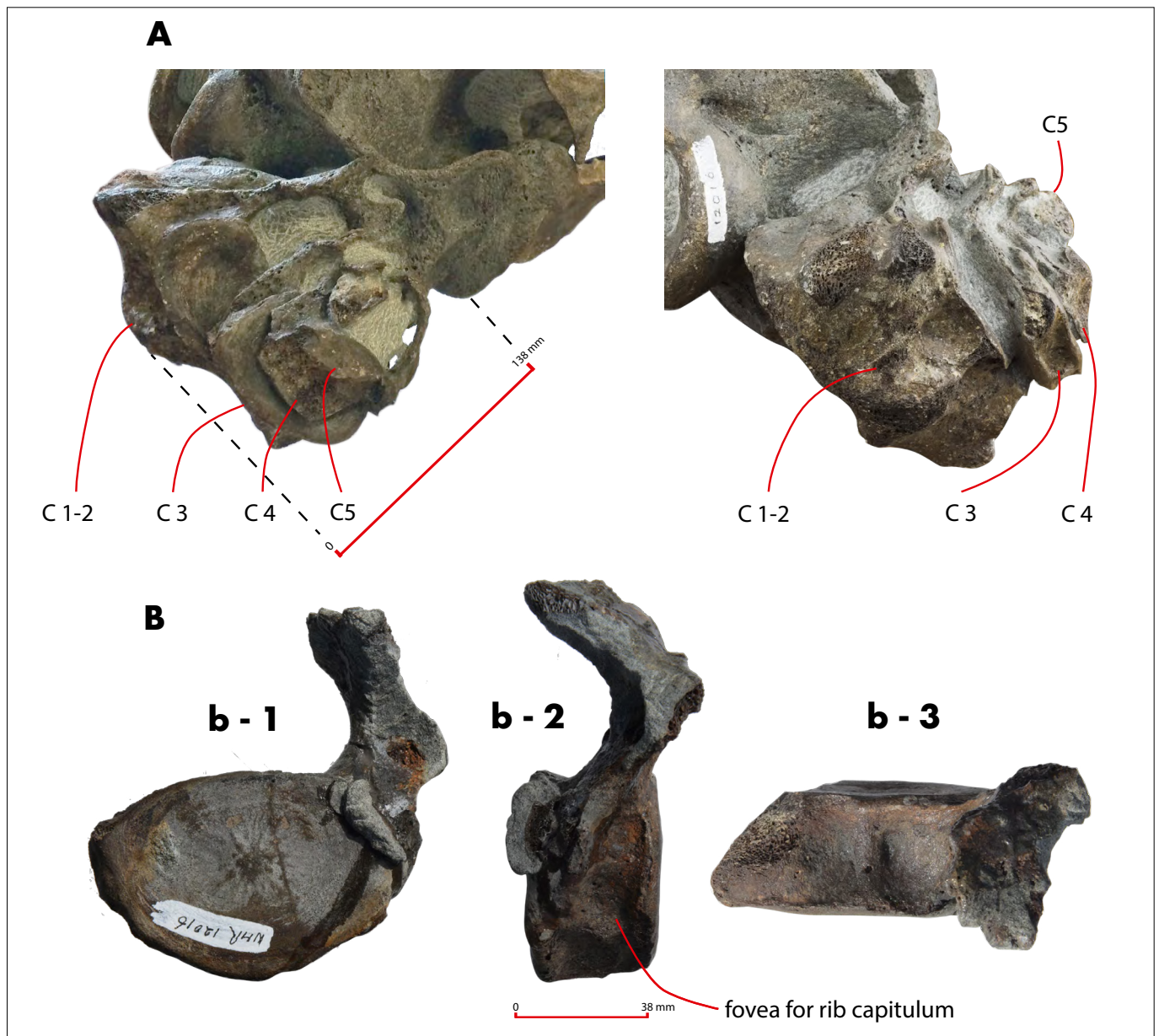


Figure 12 NMR999100012016, holotype of *Flandriacetus gijseni* gen. et sp. nov., cervical vertebrae in posterior and ventral view (A), thoracic vertebra in posterior (b-1), lateral (b-2) and dorsal view (b-3).

tubercle, both possibly for the insertion of *M. longus colli* as in *Ninoziphius* (Ramassamy 2016; Ramassamy et al. 2018). The sizes of C3 and C4 and other vertebrae are larger than similar vertebrae of *D. mojunum* and *M. gregarius* (Table 2). The first or second thoracic vertebra was detached on top of the left zygomatic arch and had to be separated from the cranium for preparation. Its vertebral centrum is completely preserved and shows a circular articulation facet of a rib (Fig. 12B2). All vertebrae show full epiphyseal fusion.

In NMR16765 the atlas and axis vertebrae are not fused to a solid complex as in NMR12016, but remain completely separated (Fig. 4A, 4C, Fig. 9, Fig. 12). They have – as the other cervicals – the same morphology and size as the cervical vertebrae of NMR12016 and the epiphyses are fully fused with the vertebral body. The axis of NMR16765 shows important differences with the corresponding partly preserved

axis of *M. gregarius* (MUSM 2548): the transverse processes differ in (relative) size and are orientated differently (laterally versus lateroventrally). Two anterior thoracic vertebrae are hidden behind the cervicals and ventral parts of the skull; only some lateral parts are visible, obstructing detailed observations. One of the thoracic vertebrae had to be separated from the block to allow preparation of important parts of the cranium. Traces of the anterior epiphysis remain (which was probably partly fused with the main vertebral body), while the posterior epiphysis was clearly not fused with the vertebral body. A large caudal vertebra is located on top of the right premaxillary sac fossa (Fig. 4A). Its two haemal processes can be observed ventrally and the dorsal extremity is completely preserved. The epiphyses were not fused to the vertebral centrum. The posterior surface of the vertebral centrum of the thoracic and caudal vertebrae show a pattern of relatively broad

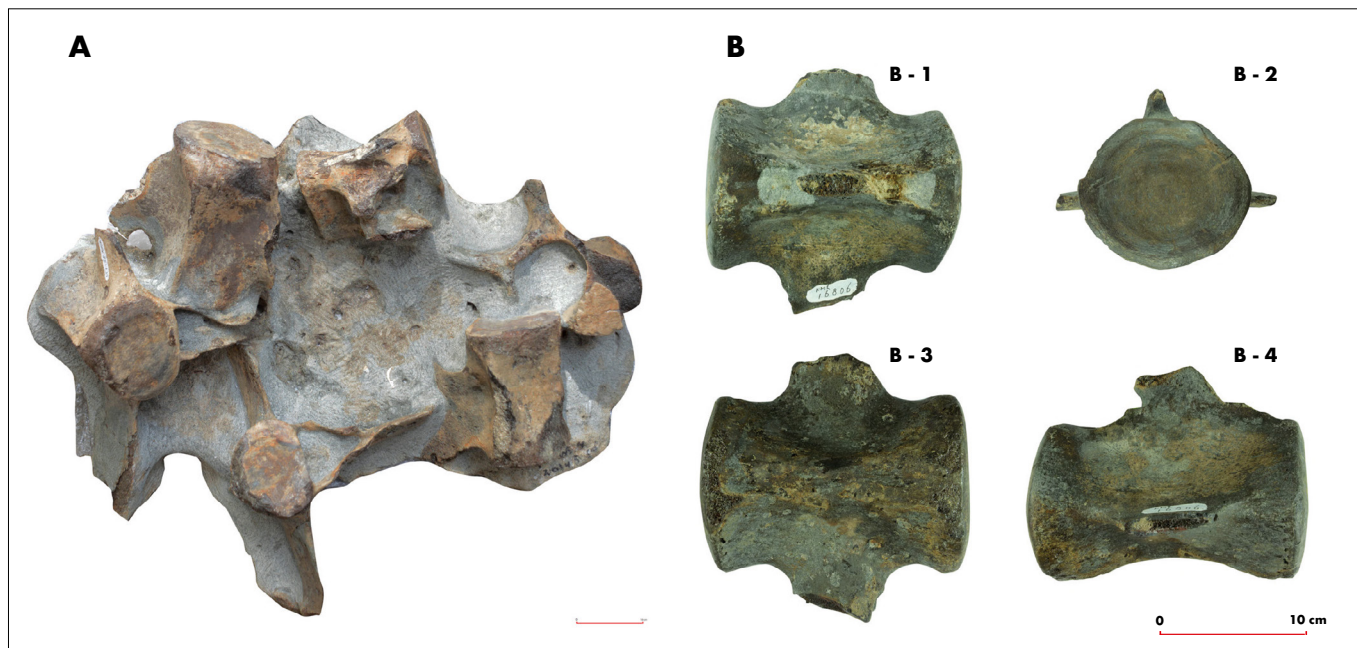


Figure 13 NMR999100151162, beaked whale vertebrae in sediment, dorsal view (A), NMR999100016806, beaked whale vertebra in dorsal (B1), anterior (B2), ventral (B3) and lateral view (B4).

ridges. An isolated epiphysial disk (from a lumbar or caudal vertebra) is preserved in a segment of the right bony nares.

Site 6D (the site where all crania were found) yielded many isolated and associated beaked whale vertebrae in sediment or with sediment attached. We may assume that – given the nature and age of the sediment, the very limited surface area of the site, and the fact that in the sediments just one beaked whale taxon was found – some (if not all) the vertebrae belong to *Flandriacetus* gen. nov. (and some might even belong to one – or more – of the described crania). We note the presence of these vertebrae but refrain from a detailed list and description because they are not directly attached to any of the crania. Some important examples are NMR151162 (two thoracic and five lumbar vertebrae), NMR16805 (four lumbar vertebrae) and NMR16806 (a large lumbar vertebra) (Fig. 13).

PHYLOGENETIC ANALYSIS

Our analysis generated one parsimonious tree, with a tree length of 95 (consistency index (CI) = 0.6842 and retention index (RI) = 0.7581) (Fig. 14, Appendix 3, Appendix 6). Although we used a slightly different approach for the analysis compared to Bianucci *et al.* (2024) (no outgroup defined, all characters treated as unordered, and all characters have equal weight), the addition of the new taxon did not substantially alter the topology of the Messapicetiformes clade. *Ninoziphius platyrostis* and *Notoziphius bruneti* (both lacking the two synapomorphies of the clade) occupy the most basal positions outside the Messapicetiformes-clade (as stated by Bianucci *et al.* 2024).

This latest analysis noted a few small differences between our new hypothesis and the one published by Bianucci *et al.* (2024): the new species *Flandriacetus gijseni* gen. et sp. nov. occupies a position just basal to the *Messapicetus* branch; *Messapicetus longirostris* and *M. gregarius* are sister species

and form a branch without *Dagonodum mojnun*; *D. mojnun* appears between the *Messapicetus* branch and *Ziphirostrum marginatum*; and *Beneziphius brevirostris* and *Beneziphius cetariensis* are sister taxa in a branch just crownwards to *Ziphirostrum* and basal to the *Aporotus* branch.

Following Bianucci *et al.* (2024), the ‘Tusciziphius-clade’ comprises the genera *Imocetus*, *Globicetus* and *Tusciziphius* with *Imocetus* being the most early diverging genus of the three. However, the polytomy formed by the genera *Globicetus* (1 species) and *Tusciziphius* (2 species) in Bianucci *et al.* (2024), is resolved in the current analysis where *Tusciziphius atlanticus* is the earliest diverging taxon of the clade.

OBSERVATIONS

Flandriacetus gen. nov. sp.

One of the key characters of the Messapicetiformes is the presence of dorsomedially elevated and fused premaxillae partly covering a deep mesorostral groove. The dorsally open part of this groove is an important difference between taxa of the clade and is one of the main features which differentiate *F. gijseni* gen. et sp. nov. from closely related taxa. In *F. gijseni* gen. et sp. nov. the open space (measured to the base of the rostrum) is 231–254 mm (n=5), for *M. longirostris* from Italy 206–230 mm (n=2), for *M. longirostris* of the Balears > 180 mm (n=1 and not completely preserved), for *M. gregarius* from Peru 163–210 mm (n=9), and for *Z. marginatum* < 100 mm (Bianucci *et al.* 2018). For most of the other members of the clade that have been described, the open space is non-existent or minimal (for example in *Beneziphius* and *Choneziphius*). Unfortunately, this important feature can only be observed in specimens with a significant part of the rostrum preserved. Combined with the fact that the skulls are not collected in situ,

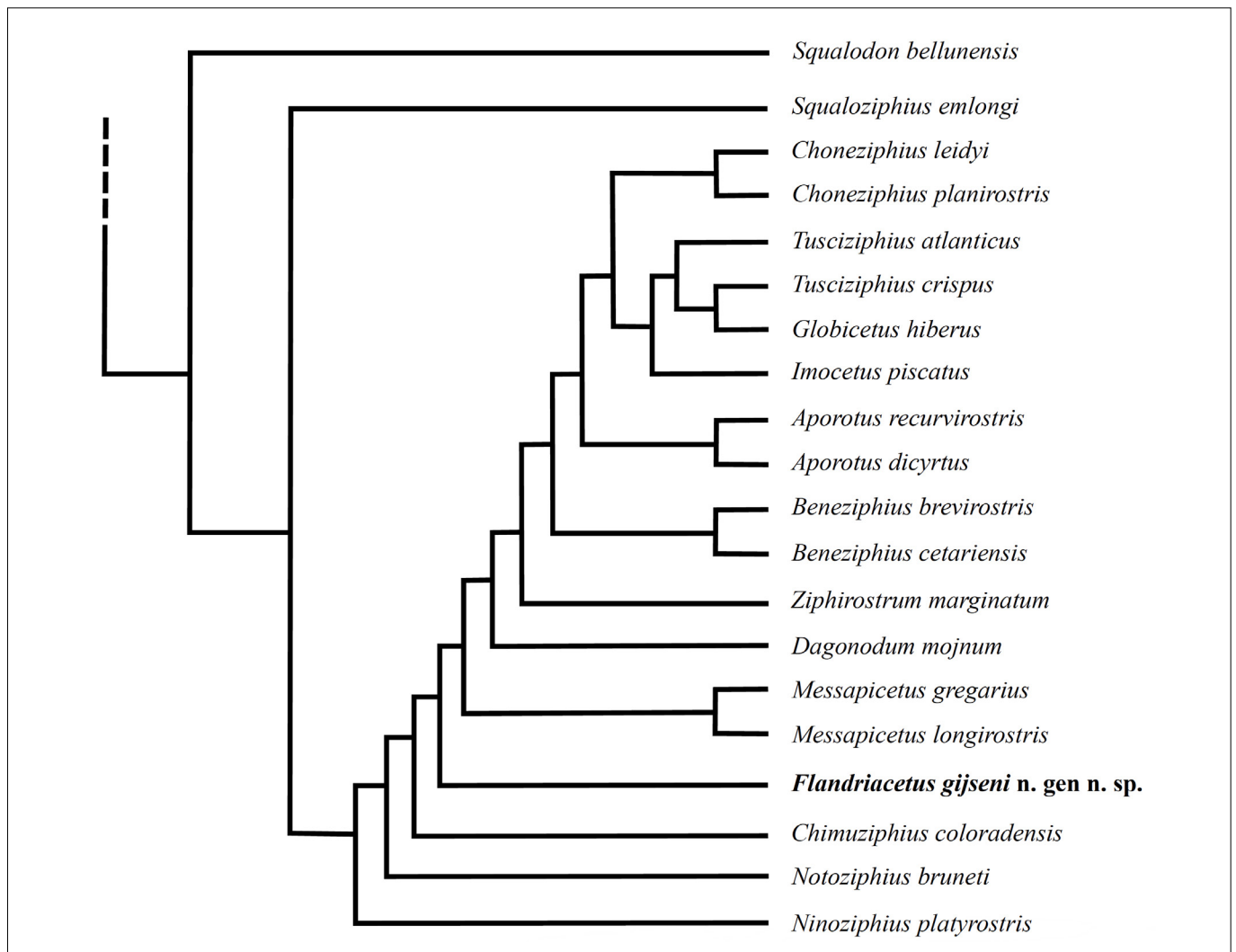


Figure 14 Tree showing the phylogenetic relationships of *Flandriacetus gijseni* gen. et sp. nov. with other Messapicetiformes, the basal stem ziphiids *Ninoziphius platyrostris* and *Notoziphius bruneti*, and two outgroup taxa (*Squalodon bellunensis* and *Squaloziphius emlongi*) (tree length = 95, CI = 0.6842, RI = 0.7581).

it urges us – despite the lack of other important morphological differences between the skulls – to identify part of the sample as *Flandriacetus* gen. nov. sp. This decision is corroborated by the observation that NMR16750 has separate atlas and axis vertebrae – as opposed to the fused atlas-axis complex of holotype NMR12016 (Fig. 4A, 4C, Fig. 9, Fig. 12). This is an important difference, because the lack of fusion of the atlas and axis of NMR16750 cannot be explained by ontogenetic processes. Although the vertebral disks of the preserved thoracic and a caudal vertebra of NMR16765 are not fused with their vertebral centrum (indicating a young or semi-adult individual), the complete fusion of the epiphyses of both atlas and axis with their vertebral centrum marks their final separation (Moran *et al.* 2015).

Gregarious lifestyle

A fossil beaked whale sample as large as the Westerschelde collection is only known from the important in situ site of Cerro Colorado in Peru (Bianucci *et al.* 2010). Some remarkable similarities are noted. In both sites multiple skulls of Tortonian

longirostrine beaked whales are preserved within in a very limited area. Some skulls are complete, show remains of functional dentition, and often the mandible is missing. Sometimes they are associated with parts of post-crania and, if so, these are usually preserved in a somewhat distorted anatomical sequence. Both faunas include cetotheres, balaenopterids, pontoporiids, seals, turtles and sharks (Bianucci *et al.* 2015; Post *et al.* 2017; Viglino *et al.* 2023). NMR16765 shows – besides the seven cervical and some first thoracic vertebrae which are positioned in a relatively correct anatomical position – a caudal vertebra dorsally positioned on the right side of the base of the rostrum. This possibly indicates a circle-wise preservation of the original carcass as is figured in a skeleton of an early delphinidan of Cerro Colorado (Bianucci *et al.* 2015). Fish (sardine) were part of the diet of *M. gregarius* and it might have had gregarious habits (Lambert *et al.* 2015). Given the general similarities between the two beaked whale taxa (morphology, numbers, environment and age) *F. gijseni* gen. et sp. nov. is supposed to have had a similar lifestyle.

Species	Ridges (one side)	Sample (n)
<i>Flandriacetus gijseni</i> gen. et sp. nov. NMR 12016	2	1
<i>Messapicetus gregarius</i> MUSM 1481	1	1
<i>Messapicetus</i> cf. <i>longirostris</i> MDM-2029	3	1
<i>Ninoziphius platyrostris</i> MNHN SAS 1628	2-3	1
<i>Hyperoodon planifrons</i> RGM H-186, 1633, 2019, 2361, 7218, 8153, 12181, 15300, 16483, 17730, 38258, 38262	0	12
<i>Berardius biardi</i> RGM 153.002	1	1
<i>Berardius anouxii</i> RGM DM 1402/21007	1	1
<i>Mesoplodon bidens</i> RGM 272, 1226, 1383, 7512, 9404, 16999, 38259, 41153	1-3	8
<i>Mesoplodon grayi</i> RGM 12340	0	1
<i>Mesoplodon layardi</i> RGM 13155, 14339	1-2	2

Table 3 Number of ridges present on the hamular process of the pterygoid in some ziphiid species.

Size

With a bizygomatic width of 331–370 mm (n=9) *F. gyseni* from the North Sea is larger than *M. gregarius* from Peru (310–313 mm, n=2). Unfortunately, bizygomatic widths from *M. longirostris* from Italy (holotype) and the Balears (MDM 2029) are not known. The bizygomatic width of some of the Westerschelde specimens reaches the value of the largest stem ziphiid of which the BZW is reported (*Chavziphius maxilloccristatus*, BZW 368 mm, Bianucci *et al.* (2016)) and implies a total minimum body length (TL) of $(\log TL = 0.92 * (\log BZW - 1.64) + 2.67) = 3.95$ metres (following Pyenson & Sponberg (2011)). Since bizygomatic widths of stem ziphiids of more than 370 mm are not (yet) reported, we may consider a length of c. 4–4.50 metres close to the maximum length which stem ziphiids are known to have reached: a far cry from the lengths of some of the extant crown ziphiids (Lambert *et al.* 2013).

Hamular process

Transverse bony ridges are observed in rare fossils of beaked whales in which the hamular processes of the pterygoid is preserved. In *Ninoziphius platyrostris* and *Messapicetus gregarius* from Peru (Ramassamy *et al.* 2018), and in a CT-scanned *M. cf. longirostris* specimen from the Balears (Bianucci *et al.* 2019) this feature is noted. In *N. platyrostris* these transverse crests might indicate a partial compartmentalisation of the sinus volume (Lambert *et al.* 2013). NMR12016, the only North Sea Basin specimen with a well preserved hamular fossa, shows two prominent bony ridges on each side of the fossa. In the large sample of *M. gregarius* only one specimen (MUSM 1481) shows one faint ridge, while the specimen from the Balears (MDM 2029) shows two or maybe even three prominent ridges. Within the family these ridges seem irregularly present: in *Hyperoodon* the bony ridges are not present at all, in *Berardius* one ridge is noted and in *Mesoplodon* species they are irregularly observed (Table 3). Extant *Ziphius cavirostris* Cuvier, 1823 and *Indopacetus pacificus* (Longman,

1926), on the other hand, show within the hamular fossa soft tissue structures with analogue transverse crests which might have replaced bony structures (Lambert *et al.* 2013). The enlarged hamular process of *M. gregarius* differs significantly from other odontocetes families, but resembles the morphology of the process in extant deep diving ziphiids (Ramassamy *et al.* 2018). *Flandriacetus* gen. nov. shows an equally enlarged hamular process (Figs. 2B, 2C, 9). Ramassamy *et al.* (2018) explain the enlargement of the hamular fossa as either 1) a combined feeding specialisation (epipelagic and benthopelagic), 2) predation avoidance, and/or 3) reversion to epipelagic feeding.

Cervical vertebrae

In the neck of NMR12016, a massive fused atlas and axis complex is followed by stocky and freely moving C3, C4 and C5 vertebrae which gradually increase in length and width, and this seems identical to the condition of the cervical complex of *Ninoziphius platyrostris* (Lambert *et al.* 2013). However, the free – or unfused – atlas and axis of NMR16765, followed by vertebrae C3–C7 which are equally solid and of gradually increasing size as in NMR12016, is the same condition noted in *Dagonodum mojnium* (Ramassamy *et al.* 2018).

The atlas and axis vertebrae of the oldest known crown ziphiid *Archaeoziphius microglenoideus* Lambert & Louwye, 2006 (from the Middle Miocene of Belgium) are not fused (Lambert & Louwye 2006). The same condition is noted in the Late Miocene *D. mojnium* and *M. gregarius* (Bianucci *et al.* 2010; Ramassamy *et al.* 2018). The Pliocene *N. urbinai* from Peru, however, shows a completely different cervical complex: the atlas and axis are fused with each other and are followed by compressed, small, slender, equally sized C3–C7 vertebrae (Lambert *et al.* 2009). This arrangement is close to the condition noted in extant ziphiids: tiny and slender C3–C7 of which at least some (or all) are fused with a massive fused atlas/axis (Van Buren & Evans 2017). Muscle attachments on



Figure 15 Global presence of longirostral stem ziphiid taxa.

the atlas and axis and other cervical vertebrae of *D. mojnium* indicate that stem ziphiids had a flexible and relatively long neck enabling the head to make stronger dorsoventral and lateral movements compared to extant ziphiids (Ramassamy *et al.* 2018). The fused robust atlas/axis and the large C3-7 vertebrae of NMR12016 and NMR16765 reach in anatomical order an estimated length of 200-215 mm. The estimated length of the neck, the robust morphology of the cervical vertebrae, the prominent supraoccipital domes of the supraoccipital, and the pronounced occipital condyles of the skull indicate a likely ability for powerful and active movements of the head.

Frontal exposure

All fossil skulls of *Flandriacetus gijseni* gen. et sp. nov. and *Flandriacetus* gen. nov. sp. show a large strip of frontal between the posterior-most lobe of the maxilla and the nuchal crest of the supraoccipital. Such an exposure of frontal is always present in young or semi-adults of most Odontoceti, but

variously and, if so – often minimally, present in adults (Van Beneden & Gervais 1880; Mead & Fordyce 2009). Except in NMR16765, all studied skulls have well fused sutures of the skull bones, indicating fully mature individuals (Mead & Fordyce, 2009). NMR16765, probably a young or semi-adult individual, also shows prominent dorsal exposure of the frontal between the maxilla and the nuchal crest (Fig. 4B). Therefore, the peculiar and constant exposure of the frontal in *Flandriacetus* gen. nov. seems not connected to ontogenetic processes. The dorsal presence of the frontal between the maxilla and the nuchal crest seems also present – albeit in a much lesser extent – in some skulls of *Messapicetus* (Bianucci *et al.* 2010; pers. ob. KP).

CONCLUSION

Based on 13 skulls from the Westerschelde estuary, a new Tortonian beaked whale genus *Flandriacetus* gen. nov. is reported. Nine skulls are attributed to the new species *F. gijseni* gen. et sp. nov., four less complete skulls are referred

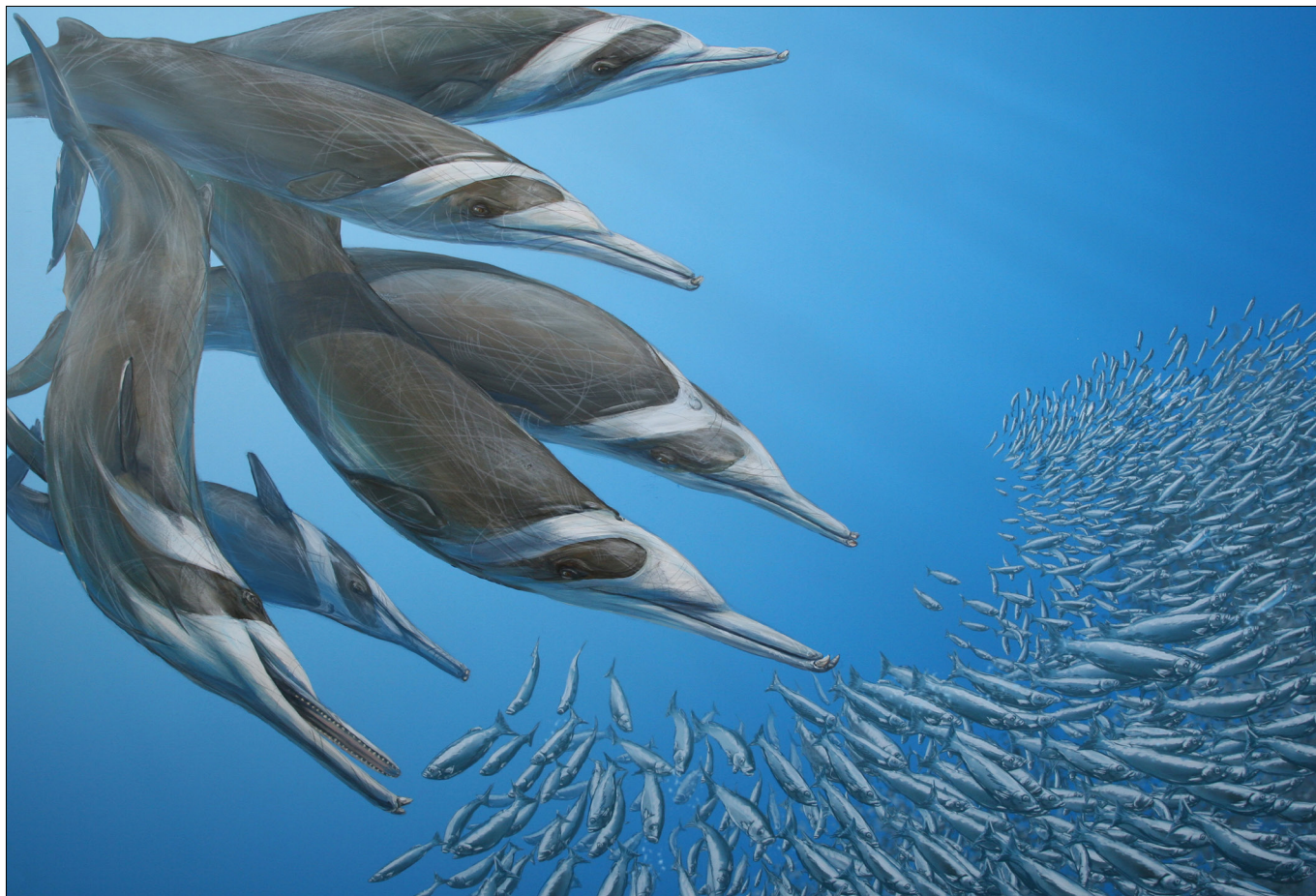


Figure 16 Hypothetical reconstruction of *Flandriacetus gijseni* gen. et sp. nov. hunting sardines. (Remie Bakker)

as *Flandriacetus* gen. nov. *Flandriacetus* gen. nov. marks – to date – the youngest appearance of longirostral stem ziphiids, reconfirms their presence in both the Southern and Northern hemispheres (Fig. 15), and corroborates the assumption that stem ziphiids never reached the huge sizes of (fossil and extant) crown ziphiids. By the presence of large numbers of individuals at a limited site – and in line with *Messapicetus gregarius* of Peru – a gregarious lifestyle of *F. gijseni* gen. et sp. nov. is proposed (Fig. 16).

ACKNOWLEDGEMENTS

First and foremost, we thank Giovanni Bianucci (University of Pisa) and Olivier Lambert (IRSNB) for information on Italian and Belgian specimens of fossil beaked whales and for many years of cooperation, pleasant discussions and wise insights on cetacean evolution. Thanks to Luc Anthonis, Bert Gijsen, Kristiaan Hoedemakers and Frederik Mollen for access to specimens in their private collections and/or detailed information; to the late Peter Moerdijk, Freddy van Nieulande and Bram Langeveld for the identification of fossil invertebrates; to Walter Aguire, Mario Urbina and Rodolfo Salas-Gismondi (MUSM) for guidance in the Ica desert of Peru and on site discussions on beaked whale evolution; to Benjamin Ramassamy for inside discussions on *Dagonodum*; to Aage Kristian Olsen Alstrup (PET-centret Aarhus Universitetshospital, Denmark) for CT scanning of NMR198032 which facilitated

preparation significantly; to Pepijn Kamminga, Natasja den Ouden and Ronald Pouwer (Naturalis Biodiversity Center) for access to their immense collections; to Nigel Larkin (University of Reading) for linguistic assistance and useful suggestions; to Malcolm Jones (PLS, UK) and Nico Janssen (GSN-TNO) for the palynological preparation of the samples; and a huge thank you to the staff of the Natural History Museum Rotterdam (especially Bram Langeveld and Kees Moeliker) for housing all these heavy and large beaked whale specimens and for allowing and facilitating our often complicated logistic operations. Last but not least, we thank the reviewers Mariana Viglino (Instituto Patagónico de Geología y Paleontología, Argentina) and Margot Nelson (Calvert Marine Museum, USA): their significant comments and suggestions greatly improved the manuscript.

REFERENCES

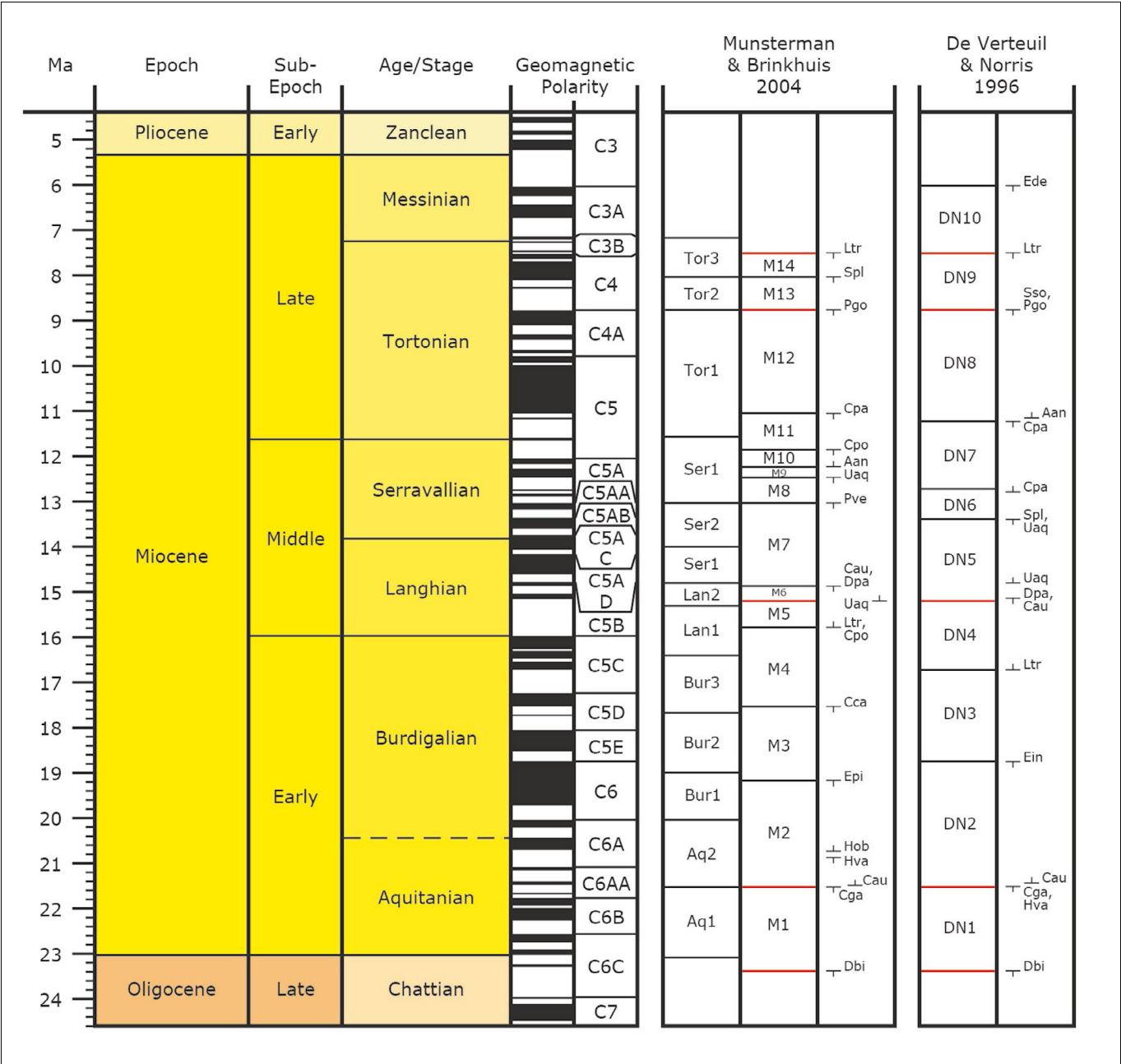
- Abbink, O.A., 1998 - Palynological investigations in the Jurassic of the North Sea region - PhD thesis, Utrecht University
- Bakker, H. & Post, K., 2020 - Records of beaked whales *Ziphirostrum* and *Aporotus* (Odontoceti, Ziphiidae) from the Miocene of The Netherlands - *Deinsea* 24: 17-26
- Bianucci, G. & Post, K., 2005 - *Caviziphius altirostris*, a new beaked whale from the Miocene southern North Sea basin - *Deinsea* 11: 1-6
- Bianucci, G., Landini, W. & Varola, A., 1992 - *Messapicetus*

- longirostris* a new genus and species of Ziphiidae (Cetacea) from the Late Miocene of "Pietra leccese" (Apulia, Italy) - *Bolletino della Società Paleontologica Italiana* 31: 261-264
- Bianucci, G., Landini, W. & Varola, A., 1994 - Relationships of *Messapicetus longirostris* (Cetacea, Ziphiidae) from the Miocene of South Italy - *Bolletino della Società Paleontologica Italiana* 33: 231-241
- Bianucci, G., Lambert, O. & Post, K., 2007 - A high diversity in fossil beaked whales (Odontoceti, Ziphiidae) recovered by trawling from the sea floor off South Africa - *Geodiversitas* 29: 5-62
- Bianucci, G., Lambert, O. & Post, K., 2010 - High concentration of long-snouted beaked whales (genus *Messapicetus*) from the Miocene of Peru - *Paleontology* 53: 1077-1098
- Bianucci, G., Miján, I., Lambert, O., Post, K. & Mateus, O., 2013 - Bizarre fossil beaked whales (Odontoceti, Ziphiidae) fished from the Atlantic Ocean floor off the Iberian Peninsula - *Geodiversitas* 35: 105-153
- Bianucci, G., Di Celma, C., Landini, W., Post, K., Tinelli, C., De Muizon, C., Gariboldi, K., Malinverno, G., Cantalamessa, A., Gioncada, A., Collareta, A., Salas Gismondi, R., Varas-Malca, R., Urbina, M. & Lambert, O., 2015 - Distribution of fossil marine vertebrates in Cerro Colorado, the type locality of the giant raptorial sperm whale *Livyatan melvillei* (Miocene, Pisco Formation, Peru) - *Journal of Maps*: 1-15; DOI 10.1080/17445647.2015.1048315
- Bianucci, G., Di Celma, C., Urbina, M. & Lambert, O., 2016A - New beaked whales from the late Miocene of Peru and evidence for convergent evolution in stem and crown Ziphiidae (Cetacea, Odontoceti) - *PeerJ* 4:e2479; DOI 10.7717/peerj.2479
- Bianucci, G., Collareta, A., Post, K., Varola, A. & Lambert, O., 2016B - A new record of *Messapicetus* from the Pietra leccese (Late Miocene, Southern Italy): antitropical distribution in a fossil beaked whale (Cetacea, Ziphiidae) - *Rivista Italiana di Paleontologia e Stratigrafia* 122 (1): 63-74
- Bianucci, G., Llacer, S., Cardona, J.Q., Collareta, A. & Florit, A.R., 2019 - A new beaked whale record from the upper Miocene of Menorca, Balearic Islands, based on CT-scan analysis of limestone slabs - *Paleontologica Polonica* 64: 291-302
- Bianucci, G., Sielfeld, W., Olguin, N.A. & Guzmán, G., 2023 - A new diminutive fossil ziphiid from the deep-sea floor off northern Chile and some remarks on the body size evolution and palaeobiogeography of the beaked whales - *Acta Palaeontologica Polonica* 68: 477-491
- Bianucci, G., Benites-Palomino, A.M., Collareta, A., Bosio, G., De Muizon, C., Merella, M., Di Celma, C., Malinverno, E., Urbina, M. & Lambert, O., 2024 - A new Late Miocene beaked whale (Cetacea, Odontoceti) from the Pisco Formation, and a revised age for the fossil Ziphiidae of Peru - *Bolletino della Società Paleontologica Italiana* 63 (1): 21-43
- Bisconti, M., Munsterman, D.K. & Post, K., 2019 - A new balaenopterid whale from the late Miocene of the Southern North Sea Basin and the evolution of balaenopterid diversity (Cetacea, Mysticeti) - *PeerJ* 7:e6915; DOI 10.7717/peerj.6915
- Bosselaers, M., 2014 - Westerschelde geeft zeer zeldzame fossiele dolfijn prijs - *Zeeland* 23: 101-102
- Brinkhuis, H., Munsterman, D.K., Sengers, S., Sluijs, A., War-
naar, J. & Williams, G.L., 2003 - Late Eocene-Quaternary dinoflagellate cysts from ODP Site 1168. Off Western Tasmania - In: Exon, N.F., Kennett, J.P. & Malone, M.J., (Eds.) - *Proceedings Ocean Drilling Project, Scientific Results* 189: 1-36
- Buono, M.R. & Cuzzuol, M.A., 2013 - A new beaked whale (Cetacea, Odontoceti) from the Late Miocene of Patagonia, Argentina - *Journal of Vertebrate Paleontology* 33(4): 986-997
- Deckers, J. & Louwe, S., 2020 - Late Miocene increase in sediment accommodation rates in the southern North Sea Basin - *Geological Journal* 55(1): 728-736
- De Verteuil, L. & Norris, G., 1996 - Miocene dinoflagellate stratigraphy and systematics of Maryland and Virginia - *Micropaleontology* 42 (Suppl.): 1-172
- Donders, T.H., Weijers, J.W.H., Munsterman, D.K., Kloosterboer-van Hoeve, M.L., Buckles, L.K., Pancost, R.D. & Brinkhuis, H., 2009 - Strong climate coupling of terrestrial and marine environments in the Miocene of northwest Europe - *Earth and Planetary Science Letters* 281(3-4): 215-225
- Dybckjær, K. & Piasecki, S., 2010 - Neogene dinocyst zonation for the eastern North Sea Basin, Denmark - *Review of Palaeobotany and Palynology* 161: 1-29
- Fensome, R.A., Williams, G.L. & MacRae, R.A., 2019 - Lentin and Williams index of fossil dinoflagellates - *AASP Contribution series* 50: 1-1173
- Fuller, A.J. & Godfrey, S.J., 2007 - A Late Miocene ziphiid (*Messapicetus* sp. Odontoceti: Cetacea) from the St. Marys Formation of Calvert Cliffs, Maryland - *Journal of Vertebrate Paleontology* 27: 535-540
- Gol'din, P.E. & Vishnyakova, K.A., 2013 - *Africanacetus* from the sub-Antarctic region: the southernmost record of fossil beaked whales - *Acta Palaeontologica Polonica* 58(3): 445-452
- Ichishima, H., 2016 - The ethmoid and presphenoid of cetaceans - *Journal of Morphology* 277: 1661-1674.
- Ichishima, H., Augustin, A.H., Toyofuku, T. & Kitazato, H., 2016. A new species of *Africanacetus* (Odontoceti: Ziphiidae) found on the deep ocean floor off the coast of Brazil - *Deep Sea Research Part II: Topical Studies in Oceanography* 146: 68-81
- Janssen, N. & Dammers, G., 2008 - Sample processing for pre-Quaternary palynology - Internal TNO report
- Knox, R.W.O.B., Bosch, J.H.A., Rasmussen, E.S., Heilmann-Clausen, C., Hiss, M., De Lugt, I.R., Kasiński, J., King, C., Köthe, A., Słodkowska, B., Standke, G. & Vandenberghe, N., 2010 - Cenozoic - In: Doornenbal, J.C. & Stevenson, A.G., (eds) - *Petroleum geological atlas of the Southern Permian Basin area*: 211-223
- Köthe, A., 2012 - A revised Cenozoic dinoflagellate cyst and calcareous nanoplankton zonation for the German sector of the southeastern North Sea Basin - *News letters on Stratigraphy* 45: 189-220
- Kuhlmann, G., Langereis, C.G., Munsterman, D.K., Van Leeuwen, R.J., Verreussel, R., Meulenkamp, J.E. & Wong, T.E., 2006 - Chronostratigraphy of Late Neogene sediments in the southern North Sea Basin and paleoenvironmental interpretations - *Palaeogeography, Paleoclimatology, Palaeoecology* 239: 426-455
- Lambert, O., 2005 - Systematics and phylogeny of the fossil beaked whales *Ziphirostrum* du Bus, 1868 and *Choneziphius*

- Duvernoy, 1851 (Mammalia, Cetacea, Odontoceti), from the Neogene of Antwerp (North of Belgium) - *Geodiversitas* 27: 443-497
- Lambert, O. & Louwey, S., 2006 - *Archaeoziphius microglenoideus*, a new primitive beaked whale (Mammalia, Cetacea, Odontoceti) from the middle Miocene of Belgium - *Journal of Vertebrate Paleontology* 26: 182-191
- Lambert, O., Bianucci, G. & Post, K., 2009 - A new beaked whale (Odontoceti, Ziphiidae) from the middle Miocene of Peru - *Journal of Vertebrate Paleontology* 29: 911-922
- Lambert, O., Bianucci, G. & Post, K., 2010 - Tusk-bearing beaked whales from the Miocene of Peru: sexual dimorphism in fossil ziphiids? - *Journal of Mammalogy* 91: 19-26
- Lambert, O., De Muizon, C. & Bianucci, G., 2013 - The most basal beaked whale *Ninoziphius platyrostris* Muizon, 1983: clues on the evolutionary history of the family Ziphiidae (Cetacea: Odontoceti) - *Zoological Journal of the Linnean Society* 167: 569-598; DOI 10.1111/zoj.12018
- Lambert, O., Collareta, A., Landini, W., Post, K., Ramassamy, B., Di Celma, C., Urbina, M. & Bianucci, G., 2015 - No deep diving: evidence of predation on epipelagic fish for a stem beaked whale from the Late Miocene of Peru - *Proceedings of the Royal Society - Biological Sciences* 282: 20151530; DOI 10.1098/rspb.2015.1530
- Lambert, O. & Louwey, S., 2016 - A new early Pliocene species of *Mesoplodon*: a calibration mark for the radiation of this species-rich beaked whale genus - *Journal of Vertebrate Paleontology* 26(1): 182-191; DOI 10.1080/02724634.2015.1055754
- Lambert, O. & Goolaerts, S., 2022 - Late Miocene survival of a hyper-longirostrine dolphin and the Neogene to Recent evolution of rostrum proportions among odontocetes - *Journal of Mammalian Evolution* 29: 99-111
- Lambert, O., Bosselaers, M. & Louwey, S., 2023 - Past beaked whale diversity in the North Sea: reappraisal through a new Miocene record and biostratigraphic analyses - *Geologica Belgica* 26(3-4): 117-126; DOI 10.20341/gb.2023.009
- Louwey, S., Head, M.J. & De Schepper, S., 2004 - Dinoflagellate cyst stratigraphy and palaeoecology of the Pliocene in northern Belgium, southern North Sea Basin - *Geological Magazine* 141(3): 353-378
- Louwey, S. & De Schepper, S., 2010 - The Miocene-Pliocene hiatus in the southern North Sea Basin (northern Belgium) revealed by dinoflagellate cysts - *Geological Magazine* 147: 760-776
- McCurry, M.R. & Pyenson, N.D., 2019 - Hyper-longirostry and kinematic disparity in extinct toothed whales - *Paleobiology* 45: 21-29
- Macleod, C.D., 2000 - Species recognition as a possible function for variations in position and shape of the sexually dimorphic tusks of *Mesoplodon* whales - *Evolution* 54: 2171-2173
- Macleod, C.D. & Herman, J.S., 2004 - Development of tusks and associated structures in *Mesoplodon bidens* (Cetacea, Mammalia) - *Mammalia* 68: 175-184
- Marx, F.G., Post, K., Bosselaers, M. & Munsterman, D.K., 2019 - A large Late Miocene cetotheriid (Cetacea, Mysticeti) from the Netherlands clarifies the status of *Tranotocetidae* - *PeerJ* 7:e6426; DOI: 10.7717/peerj.6426
- Mead, J.G. & Fordyce, R.E., 2009 - The therian skull: a lexicon with emphasis on the odontocetes - *Smithsonian Contributions to Zoology* 627: 1-248
- Miján, I., Louwey, S. & Lambert, O., 2017 - A new *Beneziphius* beaked whale from the ocean floor off Galicia, Spain and biostratigraphic reassessment of the type species - *Acta Palaeontologica Polonica* 62(1): 211-220
- Munsterman, D.K. & Brinkhuis, H., 2004 - A southern North Sea Miocene dinoflagellate cyst zonation. *Netherlands Journal of Geosciences* - 83 (4): 267-285; DOI 10.1017/S0016774600020369
- Munsterman, D.K., 2017a - The results of the palynological analysis of cemented sedimentary rocks attached to marine mammal fossils from the Neogene of the southern North Sea Basin - *TNO report R11123*: 1-49
- Munsterman, D.K., 2017b - The results of the palynological analysis of cemented sedimentary rocks attached to marine mammal fossils from the Neogene of the southern North Sea Basin - *TNO report R11369*: 1-25
- Munsterman, D.K., Ten Veen, J.H., Menkovic, A., Deckers, J., Witmans, N., Verhaegen, J., Kerstholt-Boegehold, S.J., Van de Ven, T. & Busschers, F.S., 2019 - An updated and revised stratigraphic framework for the Miocene and earliest Pliocene strata of the Roer Valley Graben and adjacent blocks - *Netherlands Journal of Geosciences* 98:e8; DOI: 10.1017/njg.2019.10
- Miján, I., Louwey, S. & Lambert, O., 2017 - A new *Beneziphius* beaked whale from the ocean floor off Galicia, Spain and biostratigraphic reassessment of the type species - *Acta Palaeontologica Polonica* 62(1): 211-220
- Moran, M.M., Bajpai, S., George, J.C., Suydam, R., Usip, S. & Thewissen, J.G.M., 2015 - Intervertebral and Epiphyseal Fusion in the Postnatal Ontogeny of Cetaceans and Terrestrial Mammals - *Journal of Mammal Evolution* 22: 93-109
- Ogg, J.G., Ogg, G. & Gradstein, F.M., 2016 - *A Concise Geologic Time Scale*: 2016 - Elsevier, Amsterdam
- Peters, M., Bosselaers, M., Post, K. & Reumer, J.W.F., 2019 - A Miocene leatherback turtle from the Westerschelde (The Netherlands) with possible cetacean bite marks: identification, taphonomy and cladistics - *Cainozoic Research* 19(2): 121-133
- Post, K. & Bosselaers, M., 2010 - Een fossiele spitssnuitdolfijn (*Ziphirostrum*) uit de Westerschelde - *Zeeland* 19: 71-73
- Post, K. & Bosselaers, M., 2017 - Cetacean fossils from a 1961 expedition at the Schelde estuary, province of Zeeland, The Netherlands - *Cainozoic Research* 17(1): 11-20
- Post, K. & Reumer, J.W.F., 2016 - History and future of paleontological surveys in the Westerschelde estuary (province of Zeeland, the Netherlands) - *Deinsea* 16: 1-9
- Post, K., Louwey, S. & Lambert, O., 2017 - *Scaldiporia vandokumi*, a new pontoporiid (Mammalia, Cetacea, Odontoceti) from the Late Miocene to earliest Pliocene of the Westerschelde estuary (The Netherlands) - *PeerJ*: 1-29, DOI 10.7717/peerj.3991
- Powell, A.J., 1992 - Dinoflagellate cysts of the Tertiary System - In: Powell, A.J. - *A stratigraphic index of dinoflagellate cysts* - Kluwer Academic Publishers, New York: 155-272
- Pyenson, N.D. & Sponberg, S.N., 2011 - Reconstructing Body

- Size in Extinct Crown Cetacea (Neoceti) using Allometry, Phylogenetic Methods and Tests from the fossil record - *Journal of Mammal Evolution* 18: 269-288
- Ramassamy, B., 2016 - Description of a new long-snouted beaked whale from the Late Miocene of Denmark: evolution of suction feeding and sexual dimorphism in the Ziphiidae (Cetacea: Odontoceti) - *Zoological Journal of the Linnean Society*: 1-29; DOI: 10.1111/zoj.12418
- Ramassamy, B., Lambert, O., Collareta, A., Urbina, M. & Bianucci, G., 2018 - Description of the skeleton of the fossil beaked whale *Messapicetus gregarius*: searching potential proxies for deep-diving abilities - *Fossil Record* 21: 11-32
- Ramassamy, B. & Lauridsen H., 2019 - A new specimen of Ziphiidae (Cetacea, Odontoceti) from the late Miocene of Denmark with morphological evidence for suction feeding behaviour - *Royal Society Open Science* 6: 191347, DOI:10.1098/rsos.191347
- Schäfer, A., Utescher, T., Klett, M. & Valdivia-Manchego, M., 2005 - The Cenozoic Lower Rhine Basin - rifting, sediment input, and cyclic stratigraphy - *International Journal of Earth Sciences (Geologische Rundschau)* 94: 621-639; DOI 10.1007/s00531-005-0499-7
- Tanaka, Y., Watanabe, M. & Kimura M., 2019 - Crown beaked whale fossils from the Chepotsunai Formation (latest Miocene) of Tomamae Town, Hokkaido, Japan - *Palaeontologia Electronica* 22.2.31A: 1-14, DOI:10.26879/897
- Van Beneden, P.J. & Gervais, P., 1880 - *Ostéographie des cétacés vivants et fossils* - Arthus Bertrand, Paris
- Van Bree, P.J.H., 1997 - Over fossiele resten van de spitsnuitdolfijn *Mesoplodon longirostris* (Cuvier, 1823) uit Zeeland - *Zeeland* 6(2): 76-78
- VanBuren, C.S. & Evans, D.C., 2017 - Evolution and function of anterior cervical vertebral fusion in tetrapods - *Biological Reviews* 92: 608-626
- Viglino, M., Valenzuela-Toro, A.M., Benites-Palomino, A., Hernández-Cisneros, A.E., Gutstein, C.S., Aguirre-Fernández, G., Vélez-Juarbe, J., Cozzuol, M.A., Buono, M.R. & Loch, C., 2023 - Aquatic mammal fossils in Latin America – a review of record, advances and challenges in research in the last 30 years - *Latin America Journal of Mammals* 18 (1):50-65
- Weber, M., 1917 - Über *Choneziphius planirostris* (G. Cuv.) aus der Westerschelde - *Sammlungen des Geologischen Reichsmuseum in Leiden* 2(8): 309-313
- Wijnker, E., Bor, T.J., Wesselingh, F.P., Munsterman, D.K., Brinkhuis, H., Burger, A.W., Vonhof, H.B., Post, K., Hoedemakers, K., Janse, A.C. & Taverne, N., 2008 - Neogene stratigraphy of the Langenboom locality (Noord-Brabant, the Netherlands) - *Netherlands Journal of Geosciences* 87: 165-180

APPENDIX 1



1 Overview of the Miocene dinocyst zonation scheme (Munsterman & Brinkhuis (2004); Ogg *et al.* (2016); Munsterman *et al.* (2019)).

APPENDIX 2

1. *Length of the rostrum* (Bianucci et al., 2010) (ordered): ratio between rostrum length and condylobasal length > 0.70 (0); ratio between 0.63 and 0.70 (1); ratio < 0.63 (2).
2. *Mesorostral groove* (Bianucci et al., 2007, modified in Bianucci et al., 2010): empty (0); filled by the mesorostral ossification of the vomer, without median suture between the lateral walls of the vomer in the rostrum base area (1); filled by the mesorostral ossification of the vomer, with median suture between the lateral walls of the vomer in the rostrum base area (2).
3. *Mesorostral groove* (Bianucci et al., 2007, modified in Bianucci et al., 2016) (ordered): open for the proximal third of the rostrum (0); anteroposteriorly elongated contact between unfused premaxillae (1); medial fusion or contact of the premaxillae extending posteriorly in front of the premaxillary foramina (2); medial fusion extending posteriorly behind and near the premaxillary foramina (3); medial fusion extending posteriorly until the bony nares (4).
4. *Prenarial basin* (Lambert, 2005c): absent (0); laterally margined by the premaxilla (1); laterally margined by a thick strip of maxilla (2).
5. *Asymmetry of the premaxillary sac fossae* (Lambert 2005c, modified in Bianucci et al., 2010): absent or weak, ratio between the widths of the left and right premaxillary fossae > 0.65 (0); moderate to high, ratio ≤ 0.65 (1).
6. *Premaxillary sac fossa laterally overhanging the maxilla* (Lambert 2005c): no (0); yes (1).
7. *Ascending process of the premaxilla in lateral view* (Bianucci et al., 2007) (ordered): rectilinear (0); slightly concave (1); concave with posterodorsal portion vertical (2); concave with posterodorsal portion partly overhanging the bony nares (3).
8. *Constriction on the ascending process of the right premaxilla (between premaxillary sac fossa and premaxillary crest)* (Bianucci et al., 2007) (ordered): roughly absent, ratio between the minimal width of ascending process of premaxilla and the width of right premaxillary crest > 0.80 (0); moderate constriction, ratio between 0.80 and 0.61 (1); strong constriction, ratio < 0.61 (2).
9. *Vertex elevation* (Bianucci et al., 2007, modified in Lambert et al., 2013) (ordered): absent to weak, ratio between the vertical distance between the dorsal margin of the maxilla at the rostrum base and the top of the vertex and the width of the premaxillary sac fossae < 0.70 (0); moderate, ratio between 0.70 and 1.0 (1); strong, ratio > 1.0 (2).
10. *Premaxillary crest direction (taken on the anterior edge in dorsal view)* (Bianucci et al., 2007, modified in Lambert et al., 2013): crest transversely directed (0); crest anterolaterally directed (1); crest posterolaterally directed (2); left crest anterolaterally directed and right crest posterolaterally directed (3). Cannot be scored for taxa lacking the premaxillary crests.
11. *Width of the premaxillary crests* (Bianucci et al., 2010) (ordered): small, ratio between the width of premaxillary crests (from the lateralmost point of the right crest to the lateralmost point of the left crest) and the width of premaxillary sac fossae < 1.0 (0); moderate, ratio from 1.0 to 1.25 (1); large, ratio > 1.25 (2). Cannot be scored for taxa lacking the premaxillary crests.
12. *Distance between premaxillary crests* (Bianucci et al., 2007): large, ratio between the minimum distance between the right and left premaxillary crests and the width of the premaxillary sac fossae > 0.25 (0); reduced, ratio ≤ 0.25 (1). Cannot be scored for taxa lacking the premaxillary crests.
13. *Nasal elongation* (Bianucci et al., 2010) (ordered): short nasal, ratio between the length of medial suture of nasals on vertex and the maximum width of nasals < 0.4 (0); elongated, ratio between 0.4 and 1.1 (1); very elongated, ratio > 1.1, with the anterior tip of nasal anterior to the premaxillary crest (2).
14. *Anteromedial excavation of the dorsal surface of the nasal* (Bianucci et al., 2007) (ordered): no (0); slight anteromedial concavity (1); well-defined anteromedial depression (2); deep excavation (3).
15. *Inclusion of the nasal in the premaxillary crest* (Bianucci et al., 2007) (ordered): no (0); for a short distance along the posteromedial angle of the premaxillary crest (1); until about halfway along the medial margin of the crest (2); reaching the anteromedial margin of the crest (3). Cannot be scored for taxa lacking the premaxillary crests.
16. *Contact between nasal and premaxillary crest* (Bianucci et al., 2007, modified in Lambert et al., 2013) (ordered): reduced, on the posterior half of the nasal (0); on more than half the length of the nasal but not the whole length (1); along the whole length of the nasal (2). Cannot be scored for taxa lacking the premaxillary crests.
17. *Interparietal or frontals as an isolated rounded protuberance on the posterior part of the vertex* (Bianucci et al., 2007): no (0); yes (1).
18. *Anteromedial margin of the supraoccipital* (Bianucci et al., 2007, modified in Lambert et al., 2013): roughly reaching dorsally the level of the vertex (0); distinctly lower than the dorsal margin of the vertex (1).
19. *Angle formed by the basioccipital crests in ventral view* (Geisler & Sanders, 2003, modified in Bianucci et al., 2010): < 50° (0); ≥ 50° (1).
20. *Fan-shaped posterior bullar facet of the periotic* (Bianucci et al., 2010): no (0); yes (1).
21. *Transverse thickening of the anterior process of the periotic* (Fordyce, 1994, modified in Bianucci et al., 2010): absent or slight thickening (0); marked thickening (1).
22. *Anterior spine of the tympanic* (Lambert, 2005b, modified in Bianucci et al., 2010) (ordered): individualized strong anterior spine (0); anterior margin pointed but without a marked thickening (1); with a more or less rectilinear anterior margin (2).
23. *Sigmoid process of the tympanic in lateral view* (Lambert 2005b, modified in Lambert et al., 2013) (ordered): high, without distinct posteroventral corner (0); posteroventral corner present and posterior margin perpendicular to long axis of the tympanic (1); posteroventral corner posteriorly projected (2).
24. *Dorsal margin of the involucrum of the tympanic cut by an indentation* (Lambert 2005b, modified in Lambert et al., 2013): absent (0); present visible in medial and/or dorsal view (1).
25. *Shape of the facets for the incus on the malleus, in posteromedial view* (Bianucci et al., 2010): elongated, ratio between the main horizontal axis length (ha) and the main vertical axis length (va) = ha/va < 1.0 (0); approximately circular, ha/va ≥ 1.0 (1).
26. *Tuberculum of the malleus* (Lambert 2005b, modified in Lambert et al., 2013): elongated tuberculum, ratio between the tuberculum and malleus lengths = lt/lm > 0.50 (0); short tuberculum, lt/lm ≤ 0.50 (1).
27. *Functional teeth in well-defined alveoli (excluding tusks)* (Bianucci et al., 2010, modified in Bianucci et al., 2016): yes (0); no (1).
28. *Tusks on the mandibles* (Bianucci et al., 2007, modified in Bianucci et al., 2010): absent (0); two enlarged pairs, apical to sub-apical (1); one enlarged pair, apical (2); one enlarged pair, not apical (3).

29. *Length of the symphyseal portion of the mandibles* (Bianucci et al., 2010, modified in Lambert et al., 2013): elongated, ratio between length of the symphyseal portion and total length: ≥ 0.35 (0); short, ratio < 0.35 (1).
30. *Thickening of the compact premaxillae (pachyosteosclerosis) on the rostrum* (ordered): absent (0); weak thickening (1); marked thickening (2); high and voluminous prominence (3).
31. *Deep excavation of the premaxillary sac fossae* (Lambert et al., 2013): absent (0); present (1).
32. *Premaxillary crest on the vertex* (Muizon, 1991, modified in Lambert et al., 2013): absent (0); present (1).
33. *Extremely ossified trapezoidal vertex* (Lambert et al., 2013): absent (0); present (1).
34. *Level of the premaxillary foramen* (Lambert et al., 2013) (ordered): distinctly anterior to the antorbital notch (0); roughly at the level of the antorbital notch (1); distinctly posterior to the antorbital notch (2).
35. *Hamular fossa of the pterygoid sinus* (Lambert et al., 2013): small, not reaching anteriorly the antorbital notch (0); wide, extending anteriorly on the palatal surface of the rostrum (1).
36. *Apices of the right and left hamular processes of the pterygoids* (Lambert et al., 2013) (ordered): contact medially, forming together a medial point posteriorly directed (0); diverge posterolaterally, forming together a concave V-shaped posterior margin (1); as for the state 1 but with less excavated and U-shaped posterior margin (2).
37. *Excavation of the apex of the hamular process by the fossa for the hamular lobe of the pterygoid sinus* (Lambert et al., 2013): no (0); yes (1).
38. *Anteroposterior shortening of the zygomatic process of the squamosal* (Lambert et al., 2013): absent, elongated zygomatic process, ratio between the height of the process (from the anterior tip of the process to the external auditory meatus) and the length of the process (from the dorsal margin of the zygomatic process to the ventral margin of the postglenoid process) < 1.10 (0); short, ratio ≥ 1.10 (1).
39. *Ventral margin of the postglenoid process of the squamosal in lateral view* (Lambert et al., 2013, modified in Bianucci et al., 2016) (ordered): clearly more ventral than the ventral margin of the paroccipital process of the exoccipital (0); approximately at the same level as the ventral margin of the paroccipital process (1); clearly more dorsal than the ventral margin of the paroccipital process (2).
40. *Extent of the lateral tuberosity of the petiotic in ventral view* (Lambert et al., 2013): transversely short (0); laterally elongated (1).
41. *Dorsal keel on the posterior process of the petiotic* (Lambert et al., 2013): present on the whole length of the process (0); absent or poorly individualized (1).
42. *Degree of fusion of the symphysis on the mandibles* (Lambert et al., 2013): reduced to absent (0); strong, dentaries nearly completely fused (1).
43. *Shape of the section of the symphyseal portion of the mandibles* (Muizon, 1991, modified in Lambert et al., 2013): triangular, pinched in posteroventral region (0); half-circled (1).
44. *Precoronoid crest* (Fordyce et al., 2002): absent, dorsal margin of the mandible rectilinear or slightly concave from the alveolar groove to the coronoid process (0); present, dorsal margin distinctly convex (1).
45. *Stomach anatomy* (Mead, 2007) (unordered): one main stomach and one pyloric stomach (0); two main stomachs and one pyloric stomach (1); two main stomachs and two pyloric stomachs (2). This character could only be coded for the extant ziphiids.
46. *Pairs of double-headed ribs* (Lambert et al., 2013): 8 or more (0); less than 8 (1).
47. *Anteroposterior length of the temporal fossa* (Lambert et al. 2015, modified in Bianucci et al., 2016) (ordered): ratio between horizontal length of the temporal fossa and the length of the neurocranium > 0.44 (0); ratio from 0.44 to 0.35 (1); ratio < 0.35 (2).
48. *Dorsal infarorbital foramina on the maxilla near the base of the rostrum* (Bianucci et al., 2016): cluster of three or more relatively small foramina (0); one large foramen sometimes associated to other, significantly smaller foramina (1).
49. *Excrescences on the dorsal surface of the maxilla on the posterior half of the rostrum* (Bianucci et al., 2016): no (0); yes (1).
50. *Posterior transverse narrowing of nasals and frontals at the vertex narrower than the nasals: absent* (Bianucci et al., 2016): (0); present (1)
51. *Fusion of cervical vertebrae in adult specimen* (Bianucci et al., 2016) (ordered): all cervical vertebrae free (0); 2-3 cervical vertebrae fused (1); 4-6 cervical vertebrae fused (2); 7 cervical vertebrae fused (3).
52. *Dorsal margin of each premaxillary crest sloping markedly ventrolaterally and generating an acute dorsal profile of the vertex in anterior view* (new character): absent (0); present (1). Cannot be scored for taxa lacking the premaxillary crests.
53. *Protuberant rostral maxillary crest medial to the antorbital process* (new character): absent (0); present (1); huge rostral crests converging posteromedially (2).
54. *Maxillary tubercle and prominent notch anteromedial to the antorbital notch* (modified from Ramassamy, 2016): absent (0); present (1).
55. *Protuberant vertex pointed in lateral view* (new character): absent (0); present (1).
56. *Fossa on the anterior surface of the ascending process of the premaxilla distinct from the premaxillary sac fossa* (new character): absent (0); present (1).
57. *Mesorostral groove dorsally closed at the level of the antorbital notches by the joined medial margins of the premaxillary sac fossae, forming a prominent ridge posteriorly shifted to the left, and separating the deeply concave anterior portions of the premaxillary sac fossae* (new character): absent (0); present (1).
58. *Half circle shaped anterior margin of the large right premaxillary fossa* (new character): absent (0); present (1).
59. *Narrow, deeper, obliquely oriented jugular notches* (new character): absent (0); present (1). We interpret the apparent small jugular notch combined with an unusually distant hypoglossal foramen observed in *Maiazihius* and in two crania of *Beradius arnouxi* and *Beradius minimus* respectively as due to a partial closure of the jugular notch and therefore we assign the derived status to these ziphiids as well.

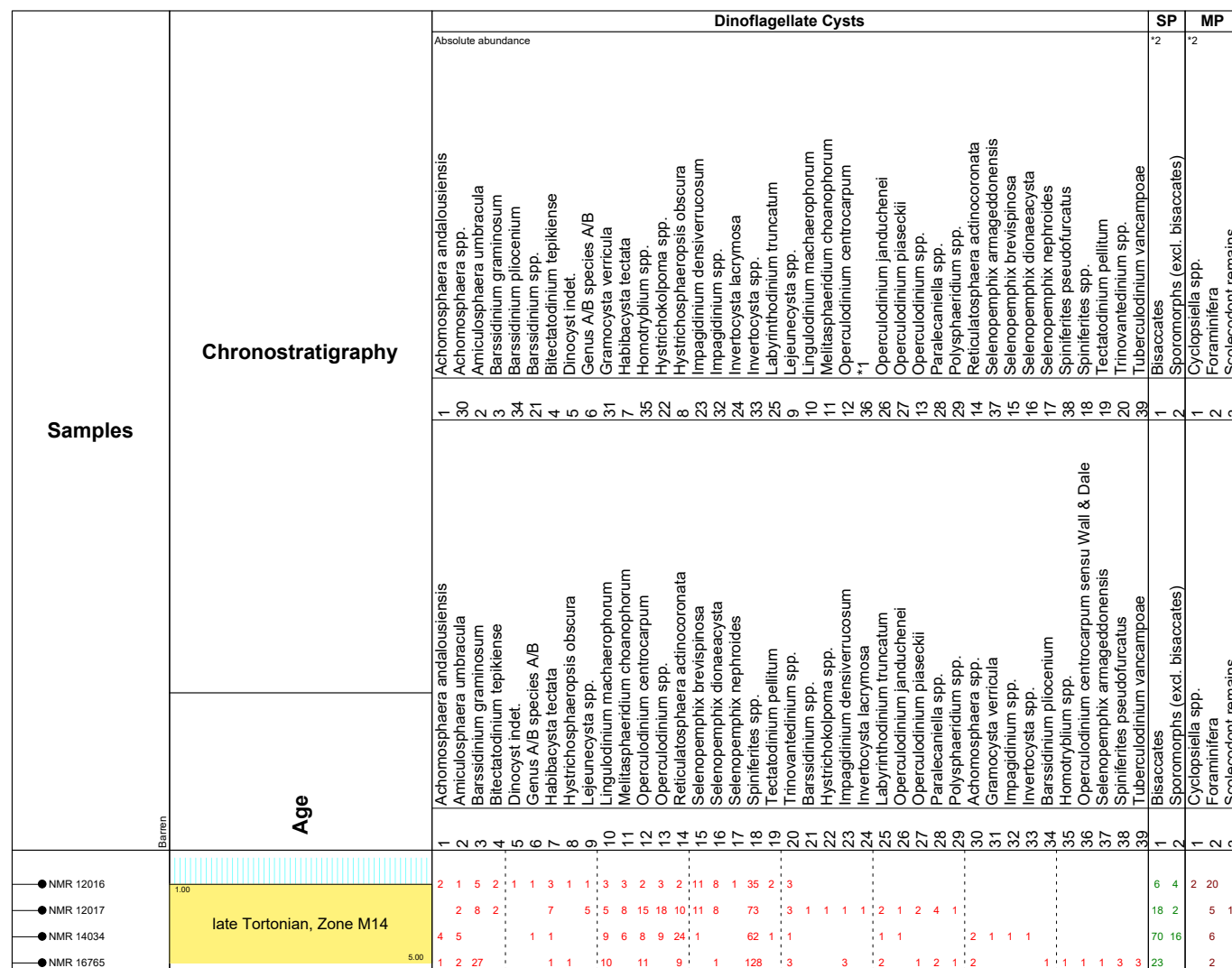
2 List of characters for the cladistic analysis of Ziphiidae (as per Bianucci et al. (2024)).

APPENDIX 3

Characters	<i>Flandriacetus gijnseni</i>	<i>Dagonodon mojunum</i>	<i>Tusciziphius atlanticus</i>	<i>Tusciziphius crispus</i>	<i>Choneziphius leidy</i>	<i>Choneziphius planirostris</i>	<i>Globicetus hiberus</i>	<i>Imocetus piscatus</i>	<i>Beneziphius brevirostris</i>	<i>Beneziphius cetariensis</i>	<i>Ziphirostrum marginatum</i>	<i>Aporotus recurvirostris</i>	<i>Aporotus dicyrtus</i>	<i>Messapicetus gregarius</i>	<i>Messapicetus longirostris</i>	<i>Chimuziphius coloradensis</i>	<i>Notoziphius bruneti</i>	<i>Ninoziphius platyrostris</i>	<i>Squalodon bellunensis</i>	<i>Squaloziphius emlongi</i>
1	0	1	1	?	2	1	1	2	2	2	1	1	1	0	0	?	?	0	0	?
2	0	0	0	0	0	0	0	0	0	0	0	0	0	0	0	0	0	0	0	0
3	2	2	4	4	4	4	4	4	3	2	2	2	2	2	2	1	?	0	0	?
4	2	2	0	0	0	0	0	1	2	2	2	2	2	2	2	0	0	0	0	0
5	0	0	1	1	1	1	1	0	0	0	0	?	0	0	0	0	0	0	0	0
6	0	0	0	0	1	1	0	0	0	0	0	0	0	0	0	0	0	0	0	0
7	1	2	3	3	2	3	3	3	2	3	2	3	1	2	2	1	1	1	0	0
8	2	?	2	2	0/1	0	2	2	1	1	1	?	0	2	2	0	0	?	0	0
9	1	1	1/2	1	2	2	1	2	2	2	2	2	2	1	1	1	1	2	0	0
10	1	1	1	1	1	1	3	3	1	1	1	1	1	1	1	1	1	1	-	0
11	1	1	1	1	1	1	1	1	1	2	1	?	1	1	1	1	1	?	-	1
12	0	1	0	0	0	0	1	0	0	0	0	0	0	0	0	0	0	0	-	-
13	1	1	1	2	1	1	2	1	1	1	1	1	1	0	0	1	1	1	0	1
14	1	1	0	1	?	?	1	1	1	1	1	0	0	1	1	1	1	0	0	0
15	0	0	0	0	0	0	0	?	0	0	0	0	0	0	0	0	0	0	-	-
16	0	0	2	2	0	0	2	2	0	0	0	0	0	0	0	0	0	0	-	-
17	0	0	0	0	0	0	0	0	0	0	0	?	0	0	0	0	0	0	0	0
18	0	0	0	0	0	0	0	0	0	0	0	?	0	0	0	0	0	0	0	0
19	1	?	1	1	?	?	?	?	?	?	?	?	?	0	0	?	?	0/1	0	1
20	?	0	?	?	?	?	?	?	?	?	?	?	?	0	?	?	?	0	0	?
21	?	0	?	?	?	?	?	?	?	?	?	?	?	0	?	?	?	0	0	?
22	?	0	?	?	?	?	?	?	?	?	?	?	?	0	?	?	?	2	0	?
23	?	?	?	?	?	?	?	?	?	?	?	?	?	2	?	?	?	1	0	?
24	?	1	?	?	?	?	?	?	?	?	?	?	?	0/1	?	?	?	1	0	?
25	?	?	?	?	?	?	?	?	?	?	?	?	?	0	?	?	?	?	0	?
26	?	?	?	?	?	?	?	?	?	?	?	?	?	1	?	?	?	?	0	?
27	0	0	1	?	1	1	1	1	0/1	0/1	0/1	1	?	0	0	?	0	0	0	?
28	?	1	?	?	?	?	?	?	?	?	?	0	?	2	?	?	?	2	0	?
29	0	0	?	?	?	?	?	?	?	?	?	0	?	0	?	?	?	0	0	?
30	1	1	3	?	2	2	3	2	2	2	1	2	2	1	1	1	0	0	0	0
31	0	0	1	1	1	1	1	1	0	0/1	0	0	0	0	0	0	0	0	0	0
32	1	1	1	1	1	1	1	1	1	1	1	1	1	1	1	1	1	1	0	1
33	0	0	1	1	0	0	1	1	0	0	0	0	0	0	0	0	0	0	0	0
34	0	0	1	?	1	0	1	2	0	0	0	0	0	0	0	0	0	0	0	2
35	1	1	1	1	1	1	1	1	?	1	1	1	1	1	1	1	1	1	0	0
36	1	?	?	0	?	?	?	?	?	?	?	?	?	1	?	?	?	1	0	0
37	1	?	?	?	?	?	?	?	?	?	?	?	?	1	?	?	?	0	0	0
38	1	?	?	1	?	?	?	?	?	?	?	?	?	1	1	?	1	1	0	0
39	2	?	?	2	?	?	?	?	?	?	?	?	?	2	2	?	2	2	0	0
40	?	0	?	?	?	?	?	?	?	?	?	?	?	0	?	?	?	0	0	?
41	?	1	?	?	?	?	?	?	?	?	?	?	?	1	?	?	?	1	0	?
42	1	1	?	?	?	?	?	?	?	?	?	?	?	1	1	?	?	1	0	?
43	1	1	1	?	?	?	?	?	?	?	?	?	?	1	1	?	?	1	0	?
44	1	1	?	?	?	?	?	?	?	?	?	?	?	1	?	?	?	1	0	?
45	?	?	?	?	?	?	?	?	?	?	?	?	?	?	?	?	?	?	?	?
46	?	?	?	?	?	?	?	?	?	?	?	?	?	?	?	?	?	0	?	?
47	1	?	1	1	?	?	?	?	?	?	?	?	?	0	0	1	1	0	0	0
48	1	?	1	0	0	0	0	0	0	0	0	0	1	0	1	0	0	0	0	0
49	0	0	0	?	1	1	0	0	1	1	0	0	0	0	0	0	0	0	0	0
50	0	0	0	0	0	0	0	0	0	0	0	0	0	0	0	0	0	0	0	0
51	1	0	?	?	?	?	?	?	?	?	?	?	?	0	?	?	?	1	0	?
52	0	0	0	0	0	0	0	0	0	0	0	0	0	0	0	0	0	0	0	0
53	0	0	1	?	0	1	0	1	0	0	0	0	1	0	0	0	0	0	0	0
54	0	1	0	?	1	0	0	0	0	0	0	0	0	1	0	0	0	0	0	0
55	0	0	0	0	0	0	0	0	0	0	0	0	0	0	0	0	0	0	0	0
56	0	0	0	0	0	0	0	0	0	0	0	0	0	0	0	0	0	0	0	0
57	0	0	0	0	1	1	0	0	0	0	0	0	0	0	0	0	0	0	0	0
58	0	0	1	1	0	0	1	1	0	0	0	0	0	0	0	0	0	0	0	0
59	1	?	?	1	?	?	?	?	?	?	?	?	?	1	1	?	1	?	0	0

3 Data matrix of 59 characters for two outgroups (*Squalodon bellunensis* and *Squaloziphius emlongi*), the basal stem ziphiids *Notoziphius bruneti* and *Ninoziphius platyrostris*, and the 16 taxa of the Messapicetiformes (including *Flandriacetus gijnseni* gen. et sp. nov.). Except *F. gijnseni* gen. et sp. nov. and numbers in red squares the matrix follows Bianucci *et al.* (2024).

APPENDIX 4



4 Palynological distribution chart from samples NMR999100012016, NMR999100012017, NMR999100014034, NMR999100016765.

APPENDIX 5

Cranium NMR999100012016

Mollusca

Abra sp.

Leionucula haesendoncki (Nyst & Westendorp, 1839)

Pseudamussium lilli (Pusch, 1837)

Lucinoma borealis (Linnaeus, 1767)

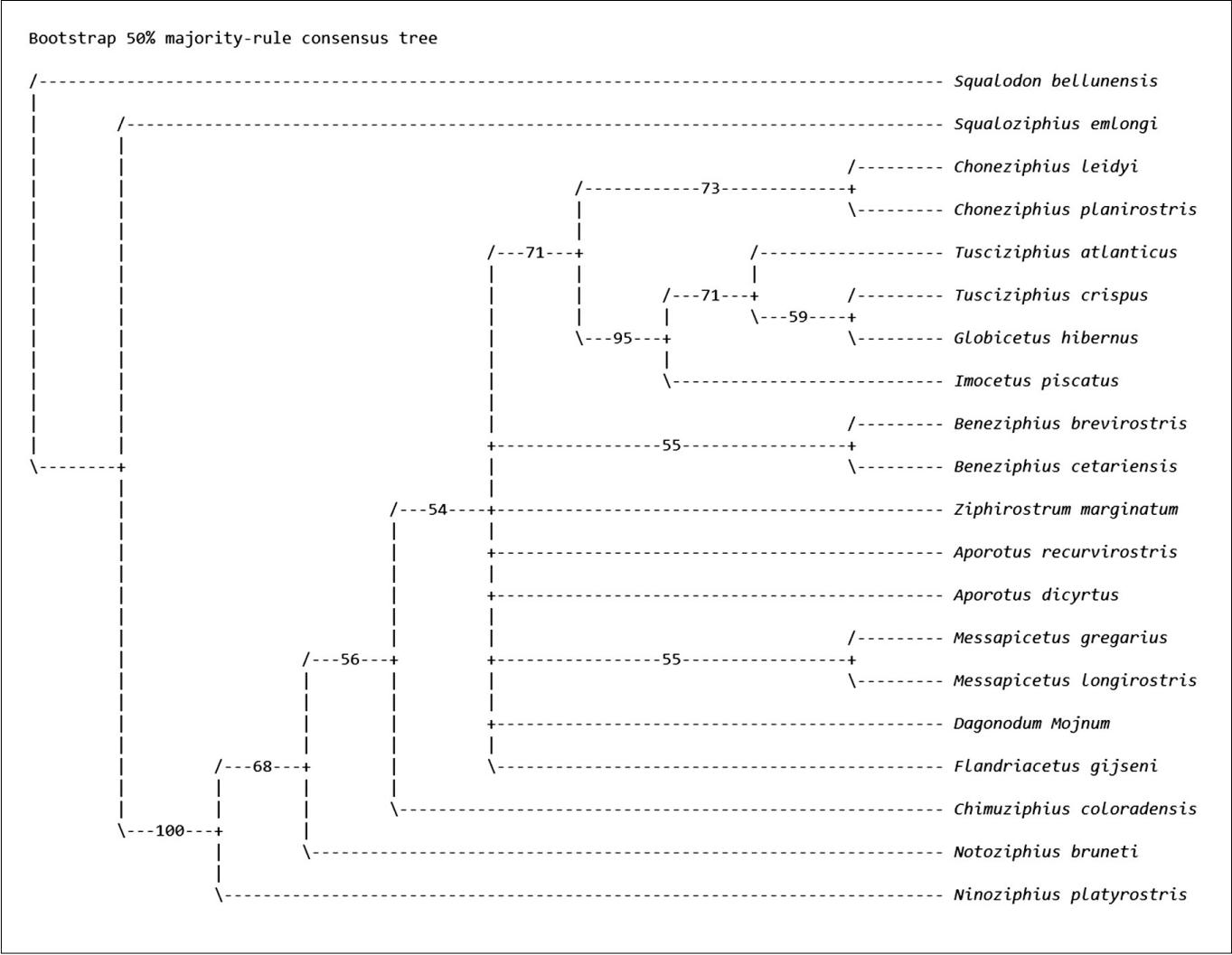
Glossus lunulatus (Nyst, 1835)

Brachiopoda


Glottidia dumortieri (Nyst, 1843)

5 Molluscs and brachiopods associated with cranium NMR999100012016.

APPENDIX 6



6 Bootstrap values of the cladogram showing the phylogenetic relationships of *Flandriacetus gijseni* gen. et sp. nov. with other Messapiceti-formes, with the basal stem ziphiids *Ninoziphius platyrostris* and *Notoziphius bruneti*, and with two outgroup taxa (*Squalodon bellunensis* and *Squaloziphius emlongi*) (tree length = 95, CI = 0.6842, RI = 0.7581).



DEINSEA - the online open-access Journal of the Natural History Museum Rotterdam publishes contributions on all aspects of natural history

editor-in-chief Jelle W.F. Reumer | **editors** Bram W. Langeveld & Cornelis W. Moeliker

design/layout Aperta, Jan Johan ter Poorten | **content, back-issues & guidelines**

www.deinsea.nl | **submissions** deinse@hetnatuurhistorisch.nl